

# CORNELL UNIVERSITY DESIGN BUILD FLY

## DESIGN REPORT 2023—2024



**CornellEngineering**



## Contents

<b>1 Executive Summary</b>	<b>4</b>
<b>2 Management Summary</b>	<b>4</b>
2.1 Team Organization . . . . .	4
2.2 Timeline and Milestones . . . . .	6
<b>3 Conceptual Design Approach</b>	<b>6</b>
3.1 Mission and Design Requirements . . . . .	6
3.1.1 Problem Statement . . . . .	6
3.1.2 General Requirements . . . . .	6
3.1.3 Mission Specific Requirements . . . . .	7
3.1.4 Mission Requirements Decomposition . . . . .	8
3.2 Scoring Sensitivity Analysis . . . . .	10
3.3 Configuration Selection and Trade Studies . . . . .	10
3.3.1 Aerodynamics Trade Studies . . . . .	10
3.3.2 Mechanical Structures Trades . . . . .	14
3.3.3 Propulsion Trade Studies . . . . .	17
<b>4 Preliminary Design</b>	<b>18</b>
4.1 Design and Analysis Methodology . . . . .	18
4.2 Aircraft Sizing Procedure . . . . .	19
4.2.1 Wing Sizing . . . . .	19
4.2.2 Empennage Sizing . . . . .	20
4.2.3 Powerplant Sizing . . . . .	21
4.3 Aircraft Analysis Procedure . . . . .	23
4.3.1 Airfoil Analysis . . . . .	23
4.3.2 Static Stability and Flight Characteristics . . . . .	24
4.3.3 Dynamic Stability Characteristics . . . . .	24
4.3.4 Turning Performance . . . . .	25
4.3.5 Uncertainty Analysis . . . . .	26
<b>5 Detailed Design</b>	<b>26</b>
5.1 Subsystem Design . . . . .	26
5.1.1 Wing Detailed Design . . . . .	26
5.1.2 Wing Integration Detailed Design . . . . .	28
5.1.3 Empennage Detailed Design . . . . .	29
5.1.4 Empennage Integration Detailed Design . . . . .	30
5.1.5 Fuselage Detailed Design . . . . .	31
5.1.6 Landing Gear Detailed Design . . . . .	32
5.1.7 Mission Package Detailed Design . . . . .	32
5.1.8 Propulsion Detailed Design . . . . .	35
5.1.9 Electronics Integration Detailed Design . . . . .	35

5.1.10 Motor Integration Detailed Design . . . . .	36
5.2 Weight and Balance . . . . .	37
5.3 Aircraft Performance . . . . .	38
5.4 Drawing Package . . . . .	38
<b>6 Manufacturing Plan</b>	<b>43</b>
6.1 Manufacturing Process . . . . .	43
6.2 Manufacturing Processes Investigated . . . . .	44
6.2.1 3D Printing . . . . .	44
6.2.2 Laser Cutting . . . . .	44
6.2.3 Adhesives . . . . .	44
6.3 Subsystem Manufacturing . . . . .	45
6.3.1 Wing Manufacturing . . . . .	45
6.3.2 Empennage Manufacturing . . . . .	45
6.3.3 Fuselage Manufacturing . . . . .	46
6.3.4 Mission Packages Manufacturing . . . . .	47
6.3.5 Electronics Hatch Manufacturing . . . . .	48
6.4 Manufacturing Milestones . . . . .	48
<b>7 Testing Plan</b>	<b>48</b>
7.1 Subsystem Tests . . . . .	48
7.1.1 Static Thrust Test . . . . .	48
7.1.2 Wingtip Tests . . . . .	49
7.2 Flight Testing Plan . . . . .	50
7.3 Flight Test Checklist . . . . .	50
<b>8 Testing Results</b>	<b>52</b>
8.1 Subsystem Test Results . . . . .	52
8.1.1 Static Thrust Test Results . . . . .	52
8.2 Flight Test Results . . . . .	52
<b>References</b>	<b>54</b>

## 1 Executive Summary

This report details the design, manufacturing, and testing of Cornell University Design Build Fly's aircraft for the 2023-2024 American Institute of Aeronautics and Astronautics Design, Build, Fly Competition, Ursula Major. The team's objective for this year's competition is to design and manufacture a remote-controlled Urban Air Mobility aircraft capable of supporting a payload including a Patient, two EMTs, a Medical Supply Cabinet (MSC), and Passengers.

Ursula Major is designed to perform three flight missions and one ground mission. Mission 1 (M1) is the Delivery Flight carrying just the crew, and it serves to demonstrate stable flight performance. Mission 2 (M2) is the Medical Transport Flight and will carry the Crew, EMTs, Patient, gurney, and MSC. Mission 3 (M3) is the Urban Taxi Flight and will carry the Crew and Passengers. The ground mission aims to demonstrate the ability to efficiently change between mission configurations.

Ursula Major is a single motor aircraft with a swiveling high wing, tricycle landing gear, a T-tail, and a tapered fuselage. A single motor was selected as it provides sufficient thrust for all missions, minimizes weight, and simplifies the electronics for the aircraft. A high wing was selected to allow for more spacious hatches and therefore easier access to the payload and better stability characteristics. Ursula Major was also designed with a swiveling mechanism, which rotates the wings in order to fit the 2.50 foot wide parking spot. A tricycle landing gear was selected as it moves the center of gravity forward which increases the static margin. A T-tail was selected so that the wake from the wing would not affect airflow over the tail. Furthermore, it prevents the tail from interfering with the wing when retracted. A tapered fuselage was chosen to reduce overall drag. Finally, a side hatch allows easy access and switching between mission configurations. The wings and fuselage are each equipped with carbon fiber spars to provide structural support for the aircraft. These spars are crucial as they sustain the majority of the lift and weight forces.

Ursula Major has a wingspan of 58 inches and root chord of 14.70 inches with a 0.80 taper ratio and an aspect ratio of 4.40. To maximize mission score, the team conducted a sensitivity analysis to determine the number of Passengers for M3 and the weight of M2 payload. Ursula Major will carry 2.43 lbs of payload for M2 and 33 Passengers for M3 with a maximum cruise speed of 83.00 feet/s. To ensure a valid takeoff, the aircraft is expected to have a takeoff distance of 17.00 feet.

The remainder of this design report provides 1) an overview of the team and team structure, outlining the team organization, workflow, and timeline, 2) a discussion of the conceptual design process, including the mission requirements, a scoring sensitivity analysis, and trade studies to determine the overall configuration, 3) the preliminary design process detailing the design and analysis methodology, how sizing was conducted, and aerodynamic analysis, 4) the detailed design of Ursula Major's subsystems, key parameters, flight performance estimates, and a CAD drawing package, and 5) a description of how manufacturing and various tests were completed, as well as results from those tests.

## 2 Management Summary

### 2.1 Team Organization

CUDBF is an undergraduate student-run project team at Cornell University with the purpose of competing annually in the AIAA Design, Build, Fly competition. Team leadership consists of two team leads and a safety officer. One team lead is responsible for the technical direction of the team by guiding design decisions and overseeing aircraft development. The other manages the logistical aspects of the team's operations, including directing recruitment

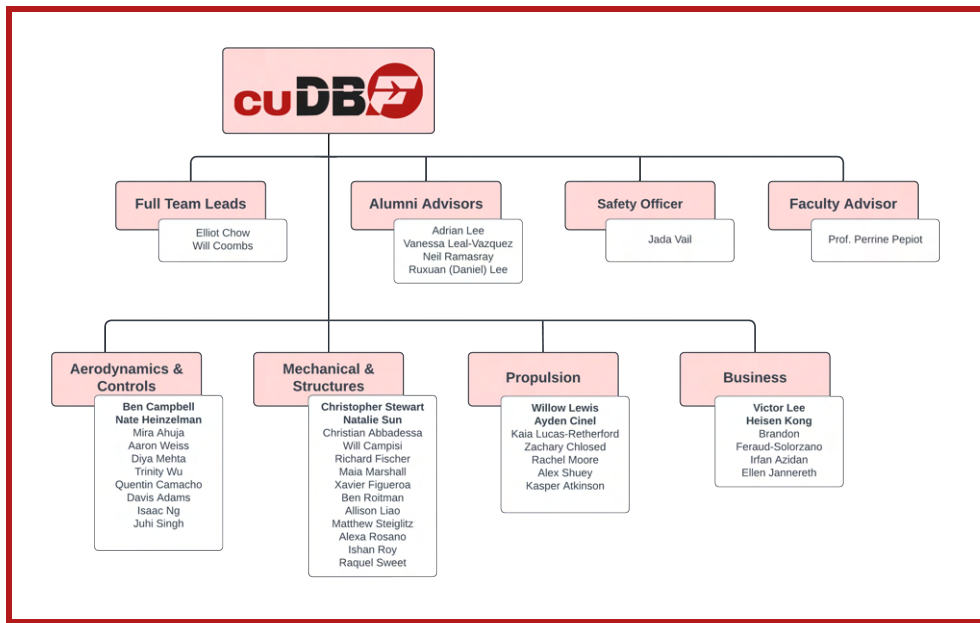


Figure 2.1.1: CU DBF's organizational structure. Subteam leads are bolded.

and managing scheduling. The safety officer ensures safe manufacturing operations and provides advice toward design decisions. The team also refers to alumni advisors to provide input on design decisions and specifications. Additionally, a faculty advisor provides technical insight and feedback during design reviews. The team is organized into four subteams, distinguished by responsibility and function as depicted in Figure 2.1.1. Each subteam has two subteam leads, responsible for directing subteam level activities and ensuring relevant subsystem requirements are met. One subteam lead is responsible for managing technical decisions, while the other manages logistics and subteam level organization. The specific role of each subteam and the individual skill sets required of the members are presented in Table 2.1.1.

Subteam	Responsibilities	Individual Skillsets
Aerodynamics and Controls	Responsible for flight performance, conducting sizing and scoring analyses. Designs and integrates the following subsystems: Wing, Empennage, Control Surfaces	Comprehensive knowledge of aerodynamic theory, proficiency in SOLIDWORKS and MATLAB, specialization in XFLR5, Xfoil, and other aerodynamics analysis tools
Propulsion	Responsible for configuration selection, development, and integration of the following subsystems: Propulsion, Avionics	Comprehensive knowledge of motor, battery, and propeller selection using ECalc; proficiency in soldering and wiring with components including receivers, ESCs, servos
Mechanical Structures	Responsible for mechanisms and structures of the aircraft. Designs and integrates the following subsystems: Fuselage, Landing Gear, Mission-Specific Mechanisms	Comprehensive knowledge of statics and mechanics of materials, proficiency in SolidWorks, MATLAB, and/or ANSYS
Business	Directs team marketing and outreach, manages team budget and purchases	Strong organizational and communication skills, familiarity with web design and social media

Table 2.1.1: Subteam Responsibilities and Skillsets

## 2.2 Timeline and Milestones

Gantt Charts are used to manage the team's deadlines and operations. A high-level Gantt Chart was created at the beginning of the academic year to keep track of important milestones and due dates. Moreover, the Gantt Chart provides a holistic overview of the design and manufacturing timeline. Figure 2.2.1 shows the Gantt Chart used for the 2023-2024 Design, Build, Fly cycle.

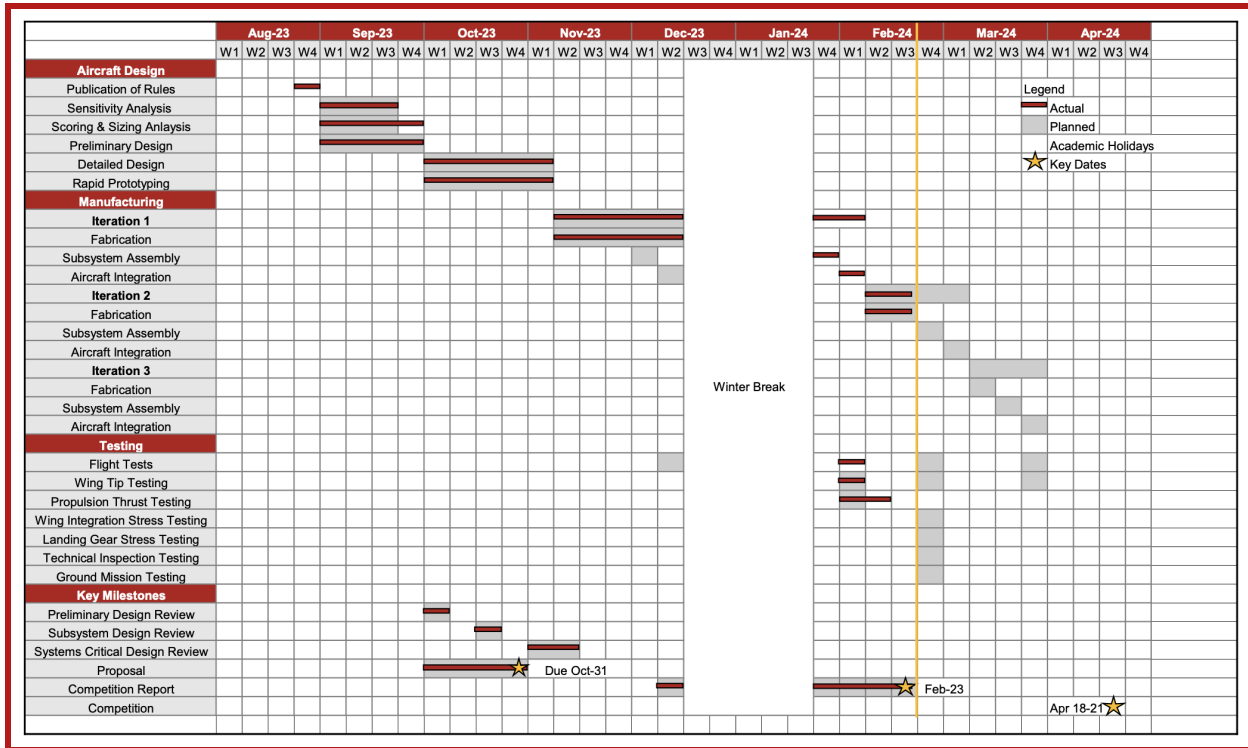


Figure 2.2.1: Gantt Chart of Planned and Actual Development Timeline

## 3 Conceptual Design Approach

### 3.1 Mission and Design Requirements

#### 3.1.1 Problem Statement

The theme of the 2023-2024 AIAA DBF competition is Urban Air Mobility. Ursula Major will undertake three flight missions and one ground mission. The missions will score the plane's transportation capabilities (M1), medical transportation (M2), urban taxiing (M3), and configuration flexibility (GM). The objective of this competition is to design, manufacture, and optimize an aircraft to perform all missions and achieve the highest mission score.

#### 3.1.2 General Requirements

Each flight mission begins in the staging box with the aircraft in its parking configuration. The ground crew is given five minutes to install the propulsion battery(ies) and put the airplane in the correct configuration based on which

mission is to be attempted. The three flight missions will have the airplane follow the flight path shown in Figure 3.1.1. In the allotted five-minute window, the airplane will have to complete either three laps or as many laps as possible, depending on the mission. The time will begin once the throttle is advanced for the first take-off attempt. To successfully gain points for the mission, the airplane will have to complete a landing after the end of the given time frame.

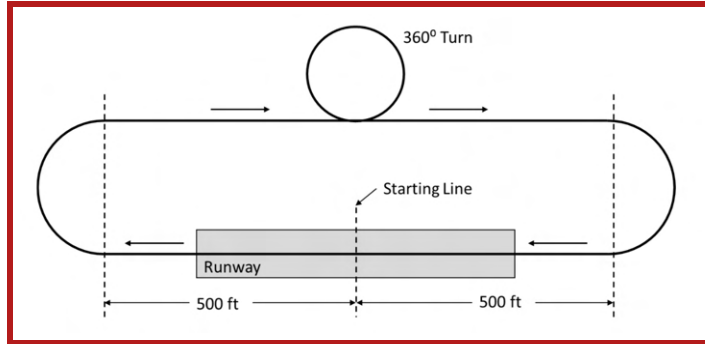


Figure 3.1.1: Competition Flight Pattern [1]

The total team score is a function of the design report score, total mission score, and participation score, where the participation score is maximized at three for attempting a flight mission. The function is given in Equation 1.

$$\text{Total Score} = \text{Design Report Score} \times (M1 + M2 + M3 + GM) + P \quad (1)$$

### 3.1.3 Mission Specific Requirements

**Mission 1: Delivery Flight** The first mission is a simulated delivery flight. For this mission, the payload is only the Crew. The goal of this mission is to complete three full laps following the flight path. The laps must be completed within five minutes which begins when the airplane's throttle is advanced. One point will be awarded after completing the laps and successfully landing. The scoring for this mission is given by Equation 2.

$$M1 = \begin{cases} 1 & \text{Successful deployment} \\ 0 & \text{Unsuccessful deployment} \end{cases} \quad (2)$$

**Mission 2: Medical Transport Flight** The second mission is a simulated medical transport flight. The payload for this mission is the Crew, EMTs, gurney, Patient, and Medical Supply Cabinet. The objective for this mission is for the plane to complete three full laps around the course as quickly as possible while carrying a heavy load. The scoring for this mission is given by Equation 3, where Max is the highest payload weight/time of all teams.

$$M2 = 1 + \left[ \frac{N_{\text{payload weight / time}}}{\text{Max}_{\text{payload weight / time}}} \right] \quad (3)$$

**Mission 3: Urban Taxi Flight** The third mission is a simulated urban taxi flight. The payload for this mission is the Crew and Passengers. The objective for this mission is for the plane to complete as many full laps around the course in five minutes as possible while carrying the highest number of Passengers possible with a low battery capacity. The

scoring for this mission is given in Equation 4, where Max is the highest laps \* passengers/battery capacity of all of teams.

$$M3 = 2 + \left[ \frac{N_{\# \text{ laps} * \# \text{passengers} / \text{battery capacity}}}{Max_{\# \text{ laps} * \# \text{passengers} / \text{battery capacity}}} \right] \quad (4)$$

**Ground Mission: Configuration Demonstration** The ground mission showcases the team's ability to swiftly adapt the plane's setup. The plane begins in its parked configuration, with nothing inside the fuselage. The Crew, EMTs, Patient, gurney, floor insert (if used), and Medical Supply Cabinet are positioned nearby. Only one crew member interacts with the plane, under pilot guidance. Upon command, they transition the plane into the first mission configuration, ensuring all components are securely in place. The process repeats with each mission's configuration with the judge verifying each setup in between. Each stage is timed separately. The scoring for this mission is given in Equation 5, where Min is the lowest mission time of all teams.

$$GM = \left[ \frac{\text{Min}_{\text{Mission Time}}}{N_{\text{Mission Time}}} \right] \quad (5)$$

### 3.1.4 Mission Requirements Decomposition

This section outlines the requirements and constraints for the four missions of the 2024 Design Build Fly Competition. They include external requirements as stipulated in the rules [1] as well as internal ones derived from those rules. In these missions, the requirements and specifications have been deconstructed and translated into a set of system requirements that the subsystems must be capable of achieving. These requirements served as a basis for configuration discussions among subteams and exploration of various design choices. Table 3.1.1 lists the requirements the aircraft must achieve.

Req	#	Requirement Description
SIZE	1	The airplane's wingspan cannot exceed five feet.
SYS	1	When in the parking configuration the airplane must fit inside a parking spot 2.50 feet wide without any components removed.
	2	The airplane shall hold the Crew for all missions, as well as the EMTs, Patient, Gurney, and Medical Supply Cabinet for M2, and Passengers for M3.
	3	The airplane shall complete a minimum of three laps within a five-minute window.
	4	The airplane shall be assembled for flight within five minutes.
	5	No component shall be released from the airplane during flight.
	6	The airplane shall take off within 20.00 feet of the start/finish line.
	7	The aircraft must be able to actuate a mechanism to transition from its parked state to its flight configuration.
AERO	1	The aircraft must generate sufficient lift for all flight missions.
	2	The mechanism transitioning the aircraft from the parking configuration to the in-flight configuration must be capable of supporting all aerodynamic loads.
	3	The control surfaces shall resist flutter while providing sufficient deflection to maintain aerodynamic control.
	4	The airplane may be of any configuration except rotary wing or lighter-than-air.
MECH	1	The Medical Supply Cabinet must have a minimum width, length, and height of 3.00, 3.00, and 3.50 inches respectively.
	2	The hinge for the hatch(es) cannot extend beyond the fuselage center line.
	3	Hatches shall not exceed a width of 6.00 inches.
	4	The aircraft shall have a single plane, horizontal floor in the passenger compartment.
	5	The Crew, EMTs, Patient on gurney, and Passengers must have a restraint system to secure them from moving.
	6	The EMTs must be alongside the Patient on the gurney.
	7	The EMTs cannot touch each other, the Patient, gurney or any part of the airplane other than the floor or insert.
	8	The Crew shall sit on a horizontal plane and be placed side-by-side without touching each other or any part of the airplane other than the floor. There must be a solid bulkhead between the Crew and Passenger compartment.
PROP	1	Brushed or brushless electric motors shall sustain flight for at least five minutes.
	2	The airplane shall use NiCad/NiMH or Lithium battery(ies).
	3	The aircraft shall have one or more motors and/or propellers.
	4	The propeller can be changed for each flight attempt.
	5	Energy for take-off shall come from the on-board propulsion battery pack(s).
	6	Each airplane will use a commercially produced propeller/blades.
	7	The airplane must have an externally accessible switch to turn on the radio control system. It cannot be internal or under a panel or hatch. An arming plug is not considered an acceptable switch. The radio control system switch must be separate from the propulsion system fuse & arming system.
	8	There can be a maximum of one battery pack connected to a propulsion system. A propulsion system consists of one battery, one externally accessible arming fuse, one or more electronic speed controllers (ESC), and one or more motors.
	9	If the ESC has a Battery Eliminator Circuit (BEC), it must be disabled.
	10	Propulsion power total stored energy cannot exceed 100 watt-hours.
	11	All battery packs must be unaltered and commercially procured as Commercial-Off-The-Shelf (COTS) battery packs. Custom battery packs will not be allowed.
	12	The maximum current rating for the Arming Fuse is 100 amps.
	13	Batteries may not be changed or charged during any mission attempt.

Table 3.1.1: Aircraft Requirements Decomposition Matrix

### 3.2 Scoring Sensitivity Analysis

Following the release of the AIAA Design Build Fly competition rules, the key parameters determining each mission's score were identified to understand the effects of varying them and to guide the development of Ursu Major. A MATLAB [2] script was developed to understand how varying these variables would affect the attainable total flight score. The team decided to investigate the M2 payload weight (represented as the payload fraction in the study and calculated per Equation 6) and the number of Passengers and battery capacity for M3. Velocity is critical in both M2 and M3 and is also considered in the sensitivity script.

$$\text{Payload Fraction} = \frac{\text{M2 Cabinet Mass}}{\text{M2 Cabinet Mass} + \text{M2 Patient/Gurney/EMT Mass} + \text{Crew Mass} + \text{Aircraft Empty Mass}} \quad (6)$$

The script utilizes the scoring equations in Section 3.1 and key aerodynamic equations to optimize the score while ensuring the plane can still take off and fly within the competition restraints. Maximum mission score estimates were approximated from the results of high-performing aircraft from the previous two years' Fly-Offs, as well as high-scoring reports from previous years. Additionally, baseline estimates were taken from previous CUDBF aircraft from the past three years. Each parameter was then modified independently and the resulting change in score was graphed.

Figure 3.2.1 shows the results of the sensitivity study. As illustrated, the minimum required battery capacity and maximum payload fraction create a range that, with the 20.00-foot take-off distance and aerodynamic validity, must be taken into account. Out of the four parameters considered, the mission score is most sensitive to velocity, as the multiplier for M2 and M3 scoring increases with each additional lap flown. Taking all these factors into account, it is found that the optimum configuration would be a battery capacity of 2400.00 mAh, while having a payload weight of 2.43 lbs for M2, and 33 Passengers for M3.

### 3.3 Configuration Selection and Trade Studies

The purpose of conceptual design and trade studies is to take the requirements set out in Table 3.1.1 and consider various aircraft designs before determining the overall aircraft shape. This aircraft shape then drives the preliminary design process, allowing the team to produce numerical values for the different subsystems before the final design is complete. To do this, trade matrices are generated to numerically weigh different options based on various parameters, including, but not limited to, ease of manufacturing, aerodynamics, overall strength, and stability. The team is then able to select optimal configurations for the aircraft build.

#### 3.3.1 Aerodynamics Trade Studies

**Wing Location Configuration** The high-wing configuration was chosen due to its ease of integration with the fuselage as well as having the most optimized takeoff field length. However, the low and mid-wings were also taken into consideration. The configurations are compared in Table 3.3.1.

Compared to the low and mid-wing, the high-wing has the highest roll stability because the center of gravity is below the wing, which is especially important for M2 and M3. However, a low-wing has a lower drag profile which makes it more efficient in sustained flight, which is important for M3's emphasis on low battery capacity. A mid-wing is a balance of both other configurations [3]. To optimize takeoff distance, a high-wing is preferred as it can implement flaps with adequate ground clearance. Low and high-wing configurations improve mission scores of M2 and M3 as these configurations allow for more storage space. Using the previous year's rib configuration for the

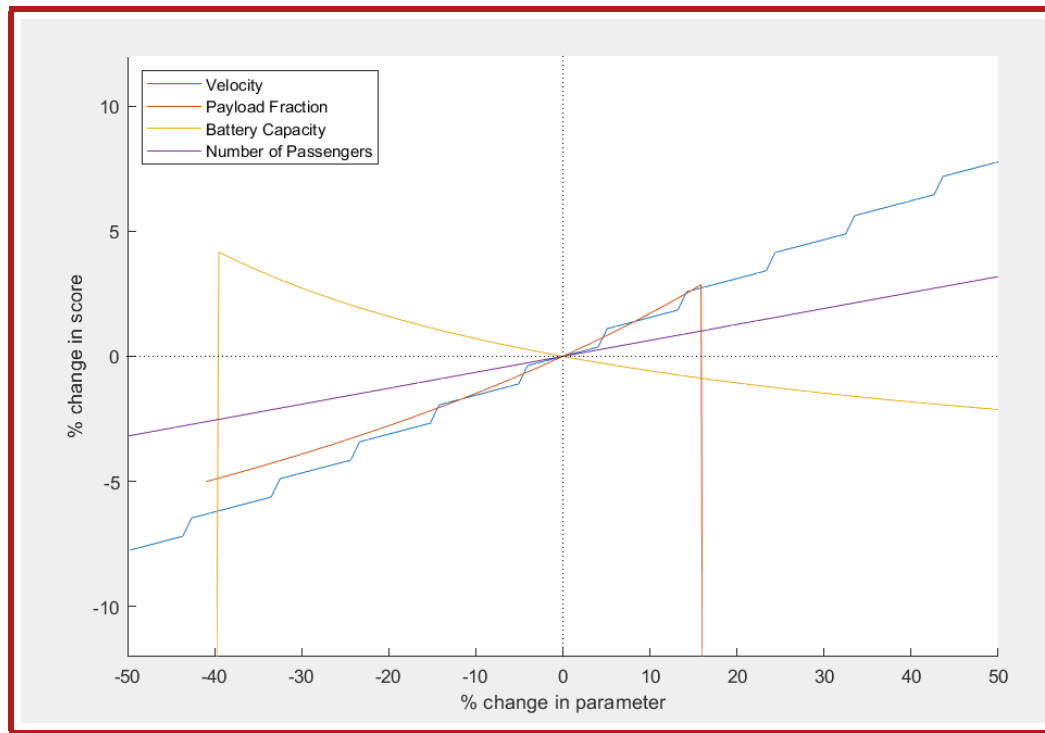


Figure 3.2.1: Sensitivity Study Results

fuselage, a mid-wing configuration would require a spar through the middle of the fuselage and make it impractical to place payloads in the fuselage.

All of the wing configurations have a similar manufacturing difficulty, but different levels of integration complexity. A low-wing may require a dihedral to offset lateral instabilities. In the past, the team experienced difficulties manufacturing an accurate dihedral due to the design complexity of the wing integration pieces. Additionally, a low-wing may interfere with the electronic components and landing gear located on the bottom of the fuselage. Integrating a mid-wing would be the most difficult because the fuselage rib design of previous years would require significant changes to allow for adequate structural stability since the current rib structure used is weakest in the center and strongest at the top and bottom.

Configuration	Aerodynamic Score	Takeoff Field Length	Mission	Manufacturing	Integration	Total Score
Low-Wing	3	1	5	3	2	14
Mid-Wing	4	3	1	3	1	12
<b>High-Wing</b>	<b>3</b>	<b>5</b>	<b>3</b>	<b>3</b>	<b>4</b>	<b>18</b>

Table 3.3.1: Wing Configuration Trade Matrix

**Taper** Tapered wings were chosen over non-tapered wings due to their higher lift generating efficiency, affecting both the takeoff field length and mission score as shown in Table 3.3.2. As the taper ratio decreases, the drag on the wings also decreases, reducing the takeoff field length. However, it is also important to consider the strength of the taper. Strongly tapered wings have an uneven lift distribution with a greater lift coefficient at the tips [4]. Therefore,

the rectangular, non-tapered wings are more stable. In terms of manufacturing, a taper is more difficult to work with when MonoKoting the surfaces. Additionally, complications arise with laser-cutting wood pieces when the taper is too aggressive. Although research has shown that a taper ratio of 0.70 is most optimal [4], a taper ratio of 0.80 was chosen to avoid the issues with lift distribution and manufacturing.

Configuration	Aerodynamics	Takeoff Field Length	Mission	Manufacturing	Total Score
Taper	4	4	4	2	14
Without Taper	3	3	3	3	12

Table 3.3.2: Taper Trade Matrix

**Flap Configuration** The 20.00-foot takeoff requirement for the competition made the team consider flaps for the wing design as shown in Table 3.3.3. One of the three options was ailerons and flaps, which is the typical control surface configuration with flaps. Following testing, the team considered if flaperons would work better for the design. This configuration would allow for greater control surface area by combining the ailerons and flaps. However, while it would be easier to manufacture fewer control surfaces, the team finds it more difficult to program flaperons as opposed to the normal flap configuration. Ultimately, the tradeoff was deemed negligible and flaperons were decided for the aircraft. A design with no flaps was considered due to its ease of manufacturing, but would make it difficult to meet the 20.00-foot take off requirement.

Configuration	Aerodynamics	Programmability	Mission	Manufacturing	Total Score
Ailerons and Flaps	4	4	3	4	15
<b>Flaperons</b>	<b>4</b>	<b>3</b>	<b>5</b>	<b>5</b>	<b>17</b>
No Flaps	3	5	1	5	9

Table 3.3.3: Flap Configuration Trade Matrix

**Control Surface Hinge Configuration** Multiple methods of attaching the control surfaces were considered, including pin hinges, nylon hinges, or wooden dowel rods, as shown in Table 3.3.4. For this year, the team wanted to utilize composite materials in the aircraft design, so it was suggested that hemicylindrical foam pieces be added to the leading edges of the control surfaces. This narrows the gap between the control surface and wing or empennage, thus making them more aerodynamic. There was initial uncertainty regarding the Robart pin hinges due to manufacturing difficulties from previous years. As a result, the team decided to explore options with control surface hinge configurations. The first idea was to use a dowel rod configuration as described in Section 5.1.1. Later, the team reexamined pin hinges and learned better practices to enhance their effectiveness, which are described in Section 5.1.3. Flat nylon hinges were also briefly considered, but they are more practical for flatter wing designs; they would not be suitable for the thicker NACA airfoil designs that the aircraft uses.

**Aircraft Configuration** Three aircraft configurations were considered for the aircraft: flying wing, conventional aircraft, and flying V. The main advantage of the flying wing configuration would be significantly reduced drag during flight conditions, but this advantage is negated by limited control surface authority in low-speed takeoff and landing conditions [5]. There is also limited storage space for cargo pieces for the flying wing [6]. The flying V configuration exhibits many of the same advantages and disadvantages as the flying wing, with the notable lack of a singular fuse-

Configuration	Image	Strength	Control	Manufacturing	Total Score
Dowel Rod		4	3	3	10
Pin Hinge		3	4	4	11
Nylon Hinge		2	3	2	7

Table 3.3.4: Control Surface Hinge Configuration Matrix

lage, limiting the size of cargo despite retaining roughly the same total cargo volume [7]. The conventional aircraft configuration was chosen due to its simplicity and familiarity, as well as the possible customization options.

Configuration	Aerodynamics	Mission	Manufacturing	Total Score
Flying Wing	3	3	3	9
<b>Conventional Aircraft</b>	<b>4</b>	<b>4</b>	<b>4</b>	<b>12</b>
Flying V	3	2	2	7

Table 3.3.5: Aircraft Configuration Matrix

**Tail Configuration** Four tail configurations were considered for the plane: conventional tail, T-tail, H-tail, and V-tail. The scores were calculated based on a high wing placement of the main wing. The conventional tail scored well, however its weakness is that the airflow over it is affected by the turbulent effects of the main wing [8]. The H-tail's primary weakness is that it weighs more than all the other tail configurations and has a more tedious structural design [8]. The V-tail scored poorly due to difficulties in maintaining aircraft longitudinal and directional stability and is more susceptible to Dutch roll tendencies than tails with separate vertical and horizontal stabilizers [8]. The T-tail's primary advantage is that it is outside of the regions of wing wake, wing downwash, and wing vortices. The T-tail requires stronger vertical structure to prevent bending moments, however the need for supports is minimized by the lessened influence from the wing effects resulting in less tail vibrations and buffeting [8].

Configuration	Aerodynamics	Mission	Manufacturing	Total Score
Conventional Tail	3	4	5	12
<b>T-Tail</b>	<b>5</b>	<b>4</b>	<b>4</b>	<b>13</b>
H-Tail	4	2	3	9
V-Tail	3	2	3	8

Table 3.3.6: Tail Configuration Matrix

**Integration Configuration** The two main configurations that would fit the 2.50 foot parking space parameter are folding wings and swiveling wings, as shown in Table 3.3.7. Both of these designs are less structurally sound than a conventional fixed-wing. However, the team concluded that no fixed wing of sufficient size could be constructed without violating the competition rules. The folding wings are weak at the point where the wings fold, and the swiveling wings have unstable rotation if not properly locked in. Swiveling wings have a greater aerodynamic score since folding wings have a gap where the wing pieces fold, affecting airflow. For mission score, folding wings take less time to switch configuration since they require a buckling or folding mechanism. Swiveling wings require bolts to be unpinned and

pinned back. On the other hand, swiveling wings allow for easier loading of passengers into the fuselage since the wings are not blocking the hatch during parking configuration. Therefore, both configurations were given the same mission score. Lastly, folding wings are more difficult to manufacture than swiveling wings. Swiveling wings require an integration piece that is 3D-printed, while folding wings require more precise manufacturing using wood. After considering these factors, swiveling wings were chosen over folding wings.

Configuration	Aerodynamics	Mission	Stability	Manufacturing	Total Score
Folding	3	4	2	5	12
<b>Swiveling</b>	<b>5</b>	<b>4</b>	<b>2</b>	<b>4</b>	<b>13</b>

Table 3.3.7: Integration Configuration Matrix

### 3.3.2 Mechanical Structures Trades

**Wing Box Configuration** With the team's decision to implement a swiveling wing design, the members responsible for the wing box (the component connecting the wings and the fuselage) of Ursa Major began to consider the specifics of the design. Due to the potentially complex nature of the mechanism, the team believed that using additive manufacturing to construct the part would provide a significant advantage. For this purpose, 3D-printed ABS and Markforged Onyx were both considered to be strong choices, but ultimately Onyx filament was chosen due to the extra strength it would lend to this crucial part of the aircraft. After this selection was made, the piece was optimized for ease of access and weight. Since the team would only have a short time to operate the mechanism during the missions, it was critical to make the process quick and efficient. Because of this, the team chose to use clevis pins to lock the wing into flight and parking configurations, as these can be inserted and removed far more easily than screws. On the other hand, the team chose to conceal the attachment points for the retention mechanism within the contour of the airfoil, whose shape would be maintained via a removable aerodynamic cover. While this made the wing box more difficult to access, it also greatly reduced its volume and saved a large amount of weight. Finally, the team chose a ball bearing to rotate the wing box around due to its small size and reliability.

Parameter	Options	Manufacturing	Weight	Ease of use	Strength	Total
Material	Wood	1	5	N/A	2	8
	Aluminum	2	1	N/A	5	8
	ABS	5	4	N/A	4	13
	<b>Onyx</b>	<b>5</b>	<b>3</b>	<b>N/A</b>	<b>5</b>	<b>13</b>
Swivel Mechanism	Turntable	4	2	5	3	14
	<b>Ball Bearing</b>	<b>4</b>	<b>3</b>	<b>5</b>	<b>4</b>	<b>16</b>
Retention Mechanism Type	<b>Clevis Pins</b>	<b>3</b>	<b>3</b>	<b>5</b>	<b>4</b>	<b>15</b>
	Screws	4	3	1	5	13
Retention Mechanism Placement	<b>Internal</b>	<b>4</b>	<b>4</b>	<b>2</b>	<b>4</b>	<b>14</b>
	External	2	1	4	3	10

Table 3.3.8: Wing Box Configuration Matrix

**Wing Box Cover** The wing box cover was created as an aerodynamic shell to fit around Ursa Major's wing box. Since this component was relatively simple, the team focused on optimizing it for low weight and ease of access. Foam was chosen for its base material, as it was extremely lightweight and capable of being shaped into complex forms. Velcro was chosen to secure the wing box cover in place as it is a simple and effective solution.

Parameter	Options	Manufacturing	Weight	Ease of access	Strength	Total
Material	Wood and Monokote	3	5	N/A	3	11
	Foam	3	5	N/A	4	12
	ABS	5	1	N/A	5	11
	CF Composite	1	3	N/A	5	9
Retention Mechanism	Clevis Pins	3	4	3	5	15
	Screws	3	4	1	5	13
	Velcro	4	5	5	2	16
	Spring Nuts	2	2	4	3	11

Table 3.3.9: Wing Box Cover Matrix

**Fuselage Configuration** The design of the fuselage can significantly affect the cost, strength, and weight of the aircraft, as well as the manufacturing timeline, replaceability, and modification of damaged components. The design must minimize weight for M3 while maximizing internal capacity for M2. The fuselage should have a good strength-to-weight ratio while being within budget.

A solid wall fuselage is made of basswood sheets. While strong and easy to manufacture, it is heavy and more expensive. In a wooden truss structure, wooden beams form a truss skeleton. While it is lightweight and cheap, it is also weak and overly complex.

A monocoque structure consists of wooden ribs, a carbon fiber spar, and a plastic skin wrap. This design is lightweight, cheap, and easy to make, but is too weak to carry out the missions. A semi-monocoque structure modifies the monocoque structure by adding wooden stringers connecting the ribs, strengthening the original design.

The fuselage material also has significant effects on the airframe's strength, cost, weight, and manufacturability. A suitable material will be light, provide sufficient structural integrity, stay within budget, and workable by the tools available to the team. The team considered two different composites for the fuselage: fiberglass and carbon fiber. Fiberglass composite is light and strong, but is also expensive and difficult to work with. Carbon fiber is marginally stronger and lighter than fiberglass composite, but is more expensive and difficult to work with. Ultimately, the strength and weight savings offered by both of these composite materials did not outweigh their cost and manufacturing difficulty. Instead, the team decided to use wood, which is cheap, easy to acquire, and manufacturable. The team used a combination of basswood for load-bearing parts and balsa wood for the rest.

Parameter	Options	Cost	Manufacturing	Mechanical Strength	Weight	Total Score
Fuselage Structure	Semi-monocoque	4	3	4	4	15
	Monocoque	4	3	1	5	13
	Solid Wall	2	4	5	2	13
	Wooden Truss	4	1	2	5	12
Fuselage Material	Wood	5	5	3	3	16
	Carbon Fiber	1	1	5	5	12
	Fiberglass Composite	2	2	4	4	12

Table 3.3.10: Fuselage Configuration Matrix

**Landing Gear Configuration** Two landing gear configurations were considered: tricycle and taildragger. Aerodynamics and stability were attributed a higher weighting factor because of their substantial effect on the plane's performance. Landing gear contributes significantly to the plane's drag which affects the plane's efficiency. Stability

is a major factor because the high winds possible in Wichita during April present a risk of crashing during takeoff and landing. A stable plane that can withstand a crosswind is imperative in preventing the plane from tipping over or a failed takeoff.

The landing gear was designed using a tricycle configuration. While the taildragger could help improve flight characteristics such as takeoff and aerodynamics, its lack of reliability in crucial areas make it susceptible to failure. Benefits of the taildragger include shorter takeoffs, less drag, and lighter weight. However, the tricycle better mitigates crosswind on takeoff and landing. The average Wichita, Kansas wind speed of almost 13.00 mph in April will jeopardize the ability of the taildragger to remain standing, thus making it an unreasonable option. The wind also exacerbates the risks of a taildragger such as nose-overs, and ground looping. The taildragger also performs worse on pavement, the surface that it will be taxiing on, which makes it even more vulnerable to the aforementioned risks.

Parameter	Options	Aerodynamics	Manufacturing	Mobility	Stability	Takeoff	Landing	Total
Landing Gear	Tricycle	3	4	5	4	3	4	3.7
	Taildragger	5	3	3	2	4	3	3.4
	Factor	0.3	0.1	0.1	0.3	0.1	0.1	

Table 3.3.11: Landing Gear Configuration Matrix

**Mission 2** For the EMT restraint system, secure transport is vital due to the risk of instability from load shifts. Laser cutting was considered, but the result was unstable overall. Velcro was considered for restraining the Crew as well. Further prototyping made it clear that a 3D-printed base would be the sturdiest and most cost-effective option. The final design consists of a rectangular base with two extruded circular holes that secure the EMTs, along with two rectangular notches at its base, that fit in pre-cut holes in the fuselage. Velcro will be used to secure the EMT restraint to the fuselage.

The second parameter of M2 requires the team to securely transport a Patient, which is larger than the rest of the crew. The first gurney design relied heavily on Velcro, but it added unnecessary weight. As a result, the shape of the patient was extruded into a 3D-printed gurney to fit the patient. However, tolerances were not exact and the design compliance with the rules was uncertain. Accordingly, a Velcro strap that fits over the patient was added to eliminate any unwanted movement. The gurney is integrated with the fuselage using two rectangular extrudes similar to the MSC, along with Velcro.

The third parameter is the MSC. The team's first design considered a hinged top, but this was difficult to manufacture. Instead, the second design had a sliding balsa plate covering the MSC that is easy to remove. 3D-printing was the most affordable and precise option for the design. The final design was a rectangular box with inserts to support two 1.10 lb weights. Stainless steel weights were chosen for their geometry, smooth texture, and accurate weight. The MSC has four extruding notches that slot into holes in the baseplate, as well as a Velcro support.

**Mission 3** M3 consists of transporting as many Passengers as possible. The Passengers must fit in the fuselage and can only touch the floor and restraint and cannot touch each other or move. Additionally, Ursa Major must be reconfigured from M2 to M3 in less than five minutes. These requirements dictated that M3 required a simple interlocking design with a quick turnaround time that also maximizes the number of Passengers.

The first parameter of M3 is to have a large Passenger capacity. After creating test Passenger configurations, the highest number of Passengers with the space available was accomplished using an alternating line method (all upright or inverted in-between), since all the space was properly utilized and capacity was doubled. The inverted

Parameter	Options	Capacity	Stability	Cost	Manufacturing	Ease of Use	Total Score
Mission 2 EMT restraint system	<b>Form-fit 3D- printed restraint</b>	5	4	5	5	5	24
	Velcro restraint system	5	3	3	5	4	20
	Laser Cut hardwood restraint	5	3	4	5	3	20
Mission 2 Gurney/patient restraint	<b>Form-fit 3D-printed Restraint with Velcro strap</b>	5	5	4	5	5	24
	Form-fit 3D-printed Restraint	5	3	5	5	5	23
Mission 2 Medical Supply Cabinet	3D-printed box with hinged top	N/A	N/A	5	3	3	11
	<b>3D-printed box with sliding Balsa cover and weight supports</b>	N/A	N/A	5	5	5	15

Table 3.3.12: Mission 2 Configuration Matrix

Passenger method was rejected due to Passenger stability concerns, the need for greater height clearance, and the required lattice support. As a result, the team decided to choose an upright alternating Passenger layout.

Next, it was important to secure the Passengers to the insert so they would not move during flight or touch each other. Three methods were considered including a lattice pattern (Fig 3.3.1), built-in backings with rubber bands (Fig 3.3.2), and a rubber backing (Fig 3.3.3). The lattice pattern was the easiest to manufacture as well as the most stable. For the rubber backing method, O-rings were originally used before the team determined that they would weigh and cost too much. Instead, a rubber sheet was purchased, cut out into strips, and placed inside the cutouts. Once the rule clarification came out, allowing for a lattice to be used, the team decided to use a combination of the rubber backings and lattice, providing a reasonable balance between cost, ease of use, and stability.

Parameter	Options	Capacity	Stability	Ease of Use	Total
Mission 3 Insert Passenger Layout	<b>Alternating</b>	4	4	4	21
	Alternating with upside down	4	2	3	18
	Singular line	2	3	4	18
Mission 3 Insert Passenger Restraint	<b>Combination</b>	4	5	5	21
	Lattice	4	4	3	21
	Rubber backing	4	2	2	15

Table 3.3.13: Mission 3 Configuration Matrix

### 3.3.3 Propulsion Trade Studies

**Motor** For the propulsion configuration, the tractor motor emerged as the best design choice from all the configurations considered. It is more aerodynamically stable and lightweight compared to the twin wing-mounted configuration. Additionally, a twin wing-mounted configuration would bring significant additional weight (as four wing halves must be manufactured) as well as take away time to assemble the aircraft to properly connect the motor wires. The tractor motor is also more efficient and easier to mount than both other designs considered. Ultimately, the pusher propeller was incompatible with the tail design, rendering it the most problematic configuration. Thus the tractor motor was chosen as the propulsion system of the aircraft.



Figure 3.3.1: M3 Lattice Pattern

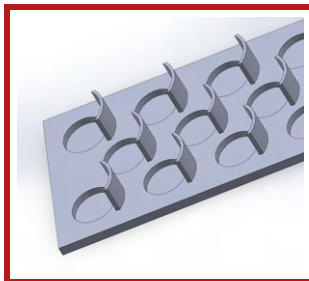


Figure 3.3.2: M3 Rubber Band Backing

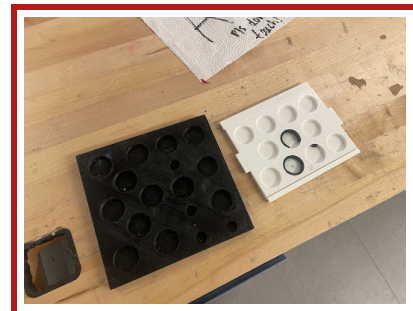


Figure 3.3.3: M3 Rubber Backing

Parameter	Options	Stability	Efficiency	Manufacturing and Integration	Total
Propulsion Configuration	Pusher Propeller	5	2	1	8
	Tractor Propeller	5	4	5	14
	Twin Wing Mounted	2	2	3	7

Table 3.3.14: Propulsion System Trade Matrix

**Electronics Integration** The integration for the plane's electronics was determined by decisions based on positioning, sizing, materials, and wiring. Table 3.3.15 details the configurations considered.

In terms of positioning, a configuration was to place the hatch that holds the propulsion system on the underside of the fuselage. It was determined that a hatch hinging on the long side of the rectangle was more optimal due to a larger angle upon opening, which in turn allows for more visibility of the electronics. Onyx was first considered as the printing material for the integration piece. Onyx offers a higher melting point, which was thought to be an important aspect when dealing with a hot ESC and main battery. ABS was chosen over Onyx for its cost-effectiveness and temperature tolerance, which allowed for the multiple iterations that were needed. The outer dimensions for the full integration piece were made to give 0.98 inches of margin space between the components and sides of the piece, and a 0.39 inch gap between the components themselves to allow for wire space. The design was later optimized, making space on the underside of the plane for the landing gear, to have no margins and have the components as close to each other while still having space for wires.

	Position	Shape	Material	Wiring
<b>Iteration 1</b>	Front hinging from bottom	Rectangle	Onyx	Towards front of inside fuselage
<b>Iteration 2</b>	Side hinging from bottom	Rectangle	ABS	Up side wall of inside fuselage
<b>Iteration 3</b>	Attached under baseplate	Rectangle with fillet	ABS	Up side wall of inside fuselage

Table 3.3.15: Electronics Integration Trade Matrix

## 4 Preliminary Design

### 4.1 Design and Analysis Methodology

The team utilizes an iterative design and analysis approach that closely mirrors the systems engineering approach used by aerospace industry professionals. The development process, including all aspects of the design, build, and flight phases, is depicted in Figure 4.1.1.

A thorough and detailed reading of the competition rules set out in August allowed all team members to understand the mission requirements, leading to the development of sub-system requirements as shown in Section 3.1. These requirements provided a list of quantitative and qualitative items that needed to be fulfilled either through design or through ground or flight testing. The subsystem requirements are further distilled in a set of trade studies that analyze the viability of different airplane configurations. The main objective of these trade studies was to define the overall airplane geometry and what the airplane should approximately look like before going into further detail about exact dimensions. Additionally, the team developed a MATLAB scoring sensitivity script to gain a better perspective of the different objectives and what should be optimized for this year's airplane. A preliminary design review concluded the conceptual design phase.

The sub-system requirements and results of the scoring sensitivity script allowed the team to progress to the preliminary design phase. Notably, a separate MATLAB sizing script, aerodynamic analysis utilizing XFLR5, and propulsion simulations using eCalc, were generated to determine quantitative benchmarks and design dimensions the airplane needed to meet. Additionally, a constraint analysis and drag predictions were used to determine our design space. These results helped refine the designs proposed in the conceptual design phase and develop subsystem and system computer-aided design (CAD) models. Subsystem and system critical design reviews allowed for team members and alumni to provide input and feedback before concluding the preliminary design phase and transitioning to fabrication and manufacturing.

Feedback from subsystem and flight tests allows the team to identify critical areas of improvement and propose solutions for future iterations. This allows an iterative design and analysis process where future iterations and prototypes improve on prior designs and lead to increased efficiency and higher flight scores.

## 4.2 Aircraft Sizing Procedure

### 4.2.1 Wing Sizing

One of the requirements for this year's competition is a short takeoff consideration, with the maximum length being only 20.00 feet. As such, it is critical that Ursa Major is light while incorporating a large lifting surface to meet this requirement. CUDBF found it useful to investigate such effects while ensuring a viable propulsion system was available. Thus, the team conducted a constraint analysis based on the takeoff distance and a fast aircraft estimated at 83.00 ft/s (a metric calculated at last year's Fly-Off). To ensure a valid takeoff and to provide a sufficient safety margin, the MATLAB script called for a 17.00-foot take-off distance, in compliance with requirement SYS 6.

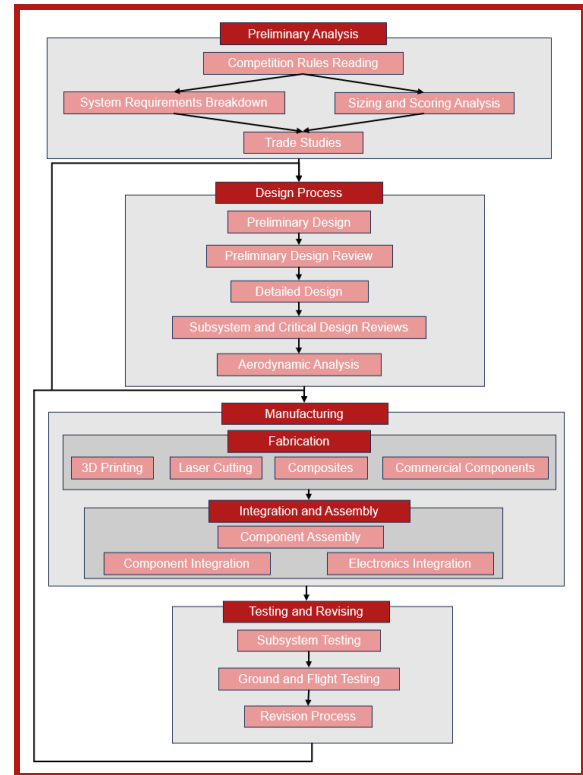


Figure 4.1.1: CUDBF Design and Manufacturing Plan

Figure 4.2.1 depicts the results of the constraint analysis with the cruising requirement derived in Gudmundsson [3] and the takeoff requirement derived from force-balance and kinematic equations (Equation 7).

$$\frac{T}{W}_{Takeoff} = \frac{WL}{g\rho\Delta x C_{z,max}} \quad (7)$$

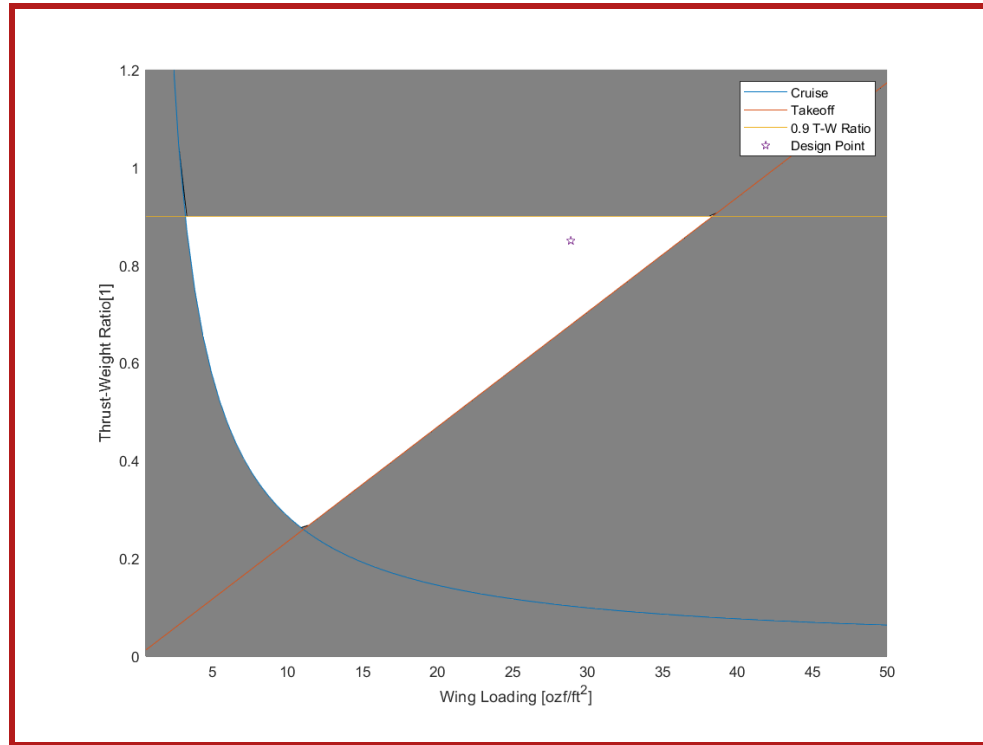


Figure 4.2.1: Constraint Analysis Results

From Figure 4.2.1, the viable design space lies between 3.3 and 38.1 ozf/ft<sup>2</sup>. To allow for a heavier payload for M2 (as justified in Section 3.2), configurations to the upper right corner were prioritized, allowing for a heavier MSC and a higher-scoring aircraft. As such, CUDBF opted for a configuration with a minimum T/W ratio of 0.85 and a wing loading of 28.9 /ft<sup>2</sup>. Following the arrival of sample patients, M2 prototype designs, and historical data from previous aircraft, the maximum takeoff weight was estimated to be about 9.65 lb, setting the desired wing area to be 5.35 ft<sup>2</sup>.

Additionally, requirement SIZE 1 imposes that the wing must have a span no larger than 60 inches. As such, to provide a factor of safety while maximizing the wingspan, the team opted for a wingspan of 58 inches. Thus, to reach the 5.35 ft<sup>2</sup> of platform area required, Ursa Major's chord was set at 13.3 inches, consequently equating the aspect ratio at 4.36. While the low aspect ratio implies a larger induced drag during cruise conditions, the priority lay in taking off in as little distance as possible.

#### 4.2.2 Empennage Sizing

The empennage is designed to provide static and dynamic stability and provide control for the pilot to climb, descend, and yaw. The tail was sized using volume coefficients as described by Raymer [9]. Approximating Ursa Major as a general aviation single-engine aircraft, equations 8 and 9, coupled with horizontal and vertical volume coefficients of

0.70 and 0.04 respectively, provided a starting point of the empennage sizing process.

$$V_H = \frac{S_H l_H}{S_w c_w} \quad (8)$$

$$V_V = \frac{S_V l_V}{S_w b_w} \quad (9)$$

A determining factor of the empennage is the distance between the empennage and the wing. To stow the aircraft in its parking configuration, it was determined that the wing would rotate about a ball bearing to keep the wing in line with the fuselage. The tail lever arm must then be large enough to accommodate this while not interfering with the vertical stabilizer. To allow for this, a 38.00-inch tail lever arm was set to allow for such flexibility. This set the required surface areas of the horizontal and vertical stabilizers. Additionally, the aspect ratios for the two stabilizers were assumed to be 2.48 and 1.44 respectively. These are within the estimates of aircraft flying similarly sized payloads from previous years. Additionally, taper was not considered due to complex manufacturability. Both stabilizers utilize a symmetrical NACA 0012 airfoil to allow for control in both directions. With the planform areas and the aspect ratios of the stabilizers selected, the geometry of the empennage was now fully defined. Table 4.2.1 summarizes the geometric parameters of the empennage.

Stabilizer	Horizontal Stabilizer	Vertical Stabilizer
Airfoil	NACA 0012	NACA 0012
Tail lever arm	38 in	38 in
Planform Area	213.4 in <sup>2</sup>	87.78 in <sup>2</sup>
Aspect Ratio	2.48	1.44
Span	23.02 in	11.24 in
Chord	9.27 in	7.81 in

Table 4.2.1: Preliminary sizing of empennage design

Following this analysis, Equation 10 [10] allowed the team to determine the aircraft's aerodynamic center mathematically. This allowed the team to determine approximately where the center of gravity of the aircraft relative to the wing should be to maintain a statically stable aircraft. This resulted in the aerodynamic center being located approximately 6.2 inches aft of the wing's leading edge. Further analysis in XFLR5 (see Section 4.3.2) attempts to validate these results.

$$\frac{l_{WF}}{l_{EF}} = \frac{S_E}{S_W} \left( \frac{\frac{2}{AR_W} - 1}{1 + \frac{2}{AR_E}} \right) \quad (10)$$

It should be noted that CUDBF is experimenting with a T-tail design this year. This allows for the vertical stabilizer and the horizontal stabilizer to take advantage of the end-plate effect and clean air respectively, accommodating a smaller tail size by about 5% [9]. However, previous CUDBF aircraft have had known difficulties with aircraft controllability, especially since the empennage has been historically small. As such, to include a safety margin, the empennage size does not reflect the 5% size reduction.

#### 4.2.3 Powerplant Sizing

The aircraft's propulsion system is constrained in multiple ways by the rules of this year's competition. As such, iterative testing using eCalc[11], coupled with market research to assess the availability of certain components, de-

terminated the best propulsion configuration.

Similar to previous years, eCalc's online calculator, propCalc, was used to size the propulsion system. This year, a Python script was developed to aid in synthesizing the eCalc data. The script uses eCalc's built-in CSV feature, which allows combinations to be saved quickly to a CSV file; following this, the results of interest can be extracted or calculated and saved to a new spreadsheet. This made the comparison of different configurations both easier and more efficient, allowing more combinations to be tested. Following the use of eCalc, in-house testing was conducted on the most promising configurations to confirm the online analysis and make a final decision.

A flight window of five minutes is specified by the competition rules, and the score calculation for M3 (given by Equation 4) favors both lower battery capacity and higher speed. In other words, the best possible propulsion system should allow the plane to achieve the maximum number of laps per unit battery capacity, while still maintaining a flight time above the flight window.

**Battery Sizing** The initial aim in sizing the propulsion system was to minimize the battery capacity while still achieving over five minutes of mixed flight time. While comparing potential configurations, one variable was isolated at a time, and combinations were recorded and processed through the code, which extracted the values of interest for comparison. Then, the combinations were compared on those values, in addition to the so-called “laps per capacity” value; this was calculated by finding the number of laps completed in a five-minute flight window and dividing it by the battery capacity in Amp-hours, using Equation 11.

$$\text{Laps/Capacity} = \frac{v \left( \frac{60\text{s}}{1\text{min}} \right) 5\text{ min}}{2500 \text{ ft/lap} (\text{Battery Capacity [mah]}) \left( \frac{1\text{Ah}}{1000\text{ mAh}} \right)} \quad (11)$$

Following this analysis, it was determined that 6s LiPo batteries gave the best performance at takeoff as they gave the motor additional rotational speed. Compiling the top-performing configurations from initial simulations, a focus range was placed around 6S1P cell configuration batteries with a capacity ranging between 2000 and 2500 milliamp hours.

**Motor and Propeller Sizing** Due to this year's high thrust requirement from the 20-foot takeoff restriction, it was quickly determined that low KV motors and large propellers. PropCalc confirmed these intuitions by suggesting configurations that would be able to meet the requirements in Section 4.2.1 with motors with low KV ratings and propellers with large diameters. While top configurations were consistently achieved by pairing either 2200 mAh or 2400 mAh LiPo battery with the Scorpion HK-4525-370 KV LOGO 690 motor, the potential configurations were restricted by commercial availability. The calculated best configurations were finalized by exploring the closest performing viable options under pricing and access constraints. These are listed in Table 4.2.2.

Component	Selected Specifications
Battery	2400 mAh 6S1P 80/120C LiPo Battery
Motors	Joker 5060-7 V3 Motor/Cobra C-4130/22 Motor
ESC	60 Amp ESC
Propeller	13 inch/15 inch propeller
Fuse	40 Amp Blade Fuse

Table 4.2.2: Viable Propulsion Options

Based on these configurations, both motors and various 13 inch and 15 inch propellers were procured for further testing. These tests are detailed further in Section 7.1.1.

## 4.3 Aircraft Analysis Procedure

### 4.3.1 Airfoil Analysis

Selecting an airfoil for the wing required the balancing of three important characteristics: lifting performance to ensure takeoff within 20 feet, low drag to allow for the highest top speeds and manufacturability. Based on these criteria, four finalist airfoils were selected: MH-114, NACA 6515, SD 7062, and USA-35B. The performance curves of these airfoils are shown in figure 4.3.1 below. The important data points were collected and are summarized in table 4.3.1. After assigning weights to the different factors, the NACA 6515 airfoil emerged as a strong candidate. Although consistently strong in all metrics, two particular strengths of this airfoil are its high CL and large physical size, providing ample space for internal components and structures.

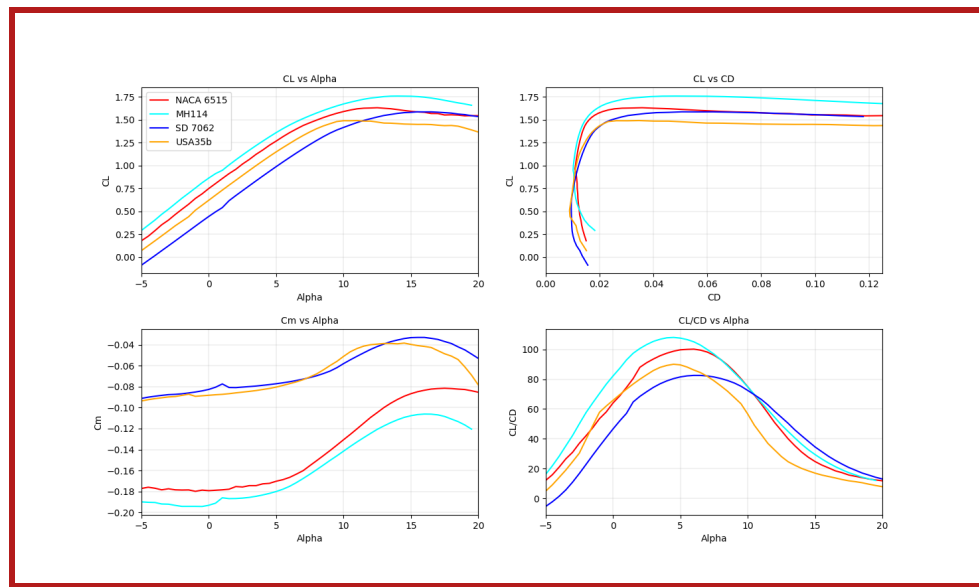


Figure 4.3.1: Clockwise From Top Left: Cl vs Alpha, Cd vs Alpha, Cm vs Alpha, Cl/Cd vs Alpha for various airfoils

Performance Factor	$C_L, \text{max}$	$C_L, 0$	Stall angle (degrees)	$C_L/C_D   \text{max}$	Manufacturability	Result
Multiplier	1	3	1	2	3	-
MH-114	4	4	3	4	1	30
<b>NACA 6515</b>	<b>3</b>	<b>3</b>	<b>2</b>	<b>3</b>	<b>4</b>	<b>32</b>
SD 7062	2	1	4	1	3	20
USA-35B	1	2	1	2	4	24

Table 4.3.1: Airfoil Comparison Table

Due to the requirement that the aircraft be able to takeoff within 20 feet, a system of flaperons were designed in order to increase the maximum coefficient of lift of the wings, allowing the aircraft to takeoff with larger loads and lower speeds. The performance of the NACA 6515 airfoil was analyzed with 20% chord flaps deflected to 10 and 20 degrees. The results of this analysis are shown below in figure 4.3.2. The inclusion of flaps increased the maximum coefficient of lift by 9.20% and 15.00% for flaps deflected 10 and 20 degrees respectively.

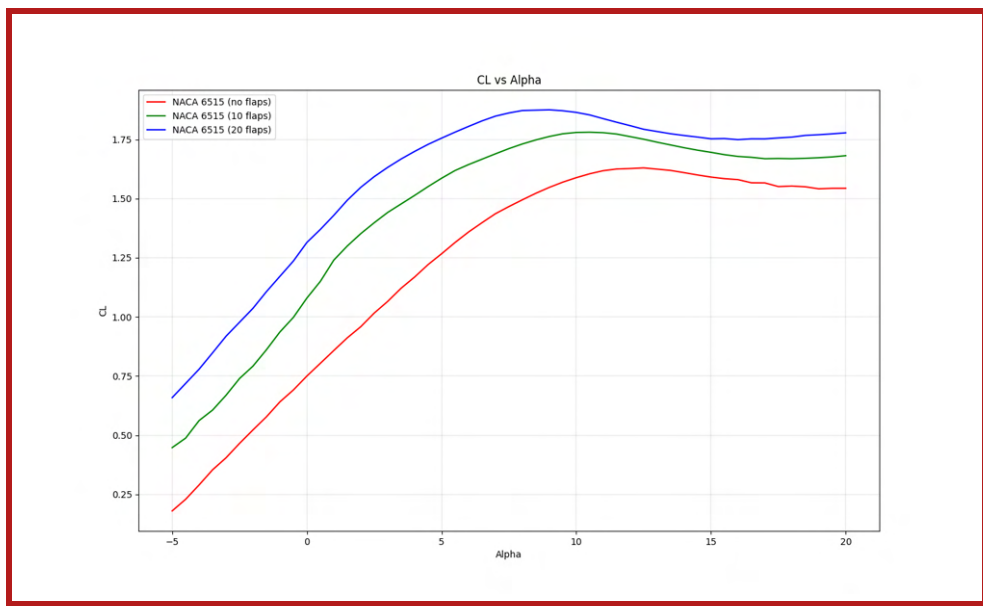


Figure 4.3.2: CL vs Alpha for NACA 6515 with no flaps, 20% chord flaps with 10 & 20 degree deflection

### 4.3.2 Static Stability and Flight Characteristics

In order to ensure that the aircraft is statically stable in flight, a static margin of -10 to -20% is desirable, allowing the aircraft to return to level flight after a disturbance while still allowing the elevator ample control authority over pitch. The mass distribution was determined from a CAD model of the aircraft. XFLR5, an open source aerodynamic analysis software, was then used to determine the flight characteristics with the center of mass in the appropriate locations for each mission. It was found that the neutral point was 7.68 inches from the leading edge of the wing. Using the desired static margin of around -15%, the optimal center of mass location was calculated to be 5.51 inch from the leading edge. Each of the missions require different cargo, so battery placement will be used to ensure that the center of mass remains in approximately the same location between the missions. Furthermore, the stability derivatives were calculated in XFLR5, as shown below in table 4.3.2. The aerodynamic performance curves for the three missions are shown in figure 4.3.3 below.

	Mass Properties		Stability Derivatives		
	Mass (lb)	Static Margin (%)	$\delta C_m / \delta \alpha$	$\delta C_l / \delta \beta$	$\delta C_n / \delta \beta$
Mission 1	7.45	-11.70	-0.30	-0.08	0.31
Mission 2	10.49	-19.20	-0.52	-0.10	0.32
Mission 3	8.99	-15.60	-0.39	-0.10	0.31

Table 4.3.2: Stability Derivatives of Ursa Major for all Missions

### 4.3.3 Dynamic Stability Characteristics

A dynamic stability analysis was conducted in XFLR5 in order to determine the flightworthiness of the aircraft. The full equations of motion of the aircraft were simplified and linearized about the steady flight condition. This allows the

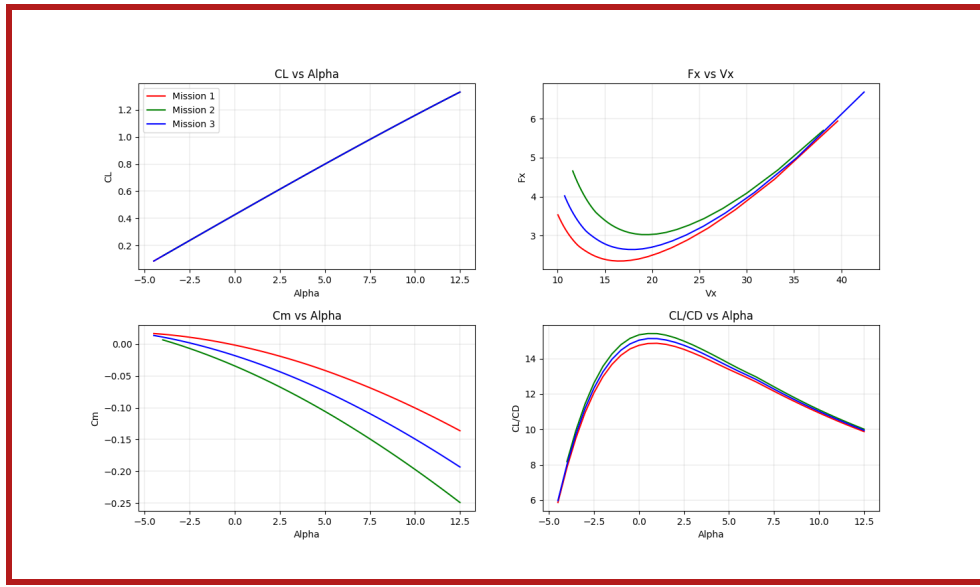


Figure 4.3.3: Aerodynamic Mission Performance for NACA 6515

response of the aircraft to disturbances in its flight condition to be modeled as the sum of contributions from various modes. Any real world disturbance will excite all modes, so in order for the aircraft to be inherently stable, all modes must be stable.

The results of the dynamic stability analysis are shown below in Table 4.3.3. All the modes are stable except for the spiral divergence. Of the stable modes, only the phugoid has a relatively long damping time and will require pilot input to hasten the return to level flight. More importantly, the pilot will need to consider the slight instability of the spiral mode with a relatively low doubling time for all three missions. This will require careful monitoring to ensure that the aircraft does not enter an unrecoverable spiral.

Mission	Parameter	Longitudinal Modes		Lateral Modes		
		Short-period	Phugoid	Roll Subsidence	Dutch Roll	Spiral Divergence
M1	Natural Frequency (Hz)	1.35	0.06	-	1.61	-
	Time to halve/double/damping ratio	$\zeta = 0.84$	$\zeta = 0.08$	$t_{1/2} = 0.04$	$\zeta = 0.26$	$t_2 = 4.68$
M2	Natural Frequency (Hz)	1.90	0.05	-	2.24	-
	Time to halve/double/damping ratio	$\zeta = 0.78$	$\zeta = 0.09$	$t_{1/2} = 0.03$	$\zeta = 0.25$	$t_2 = 8.77$
M3	Natural Frequency (Hz)	1.83	0.05	-	2.16	-
	Time to halve/double/damping ratio	$\zeta = 0.79$	$\zeta = 0.09$	$t_{1/2} = 0.03$	$\zeta = 0.25$	$t_2 = 8.24$

Table 4.3.3: Dynamic Stability Characteristics of Ursula Major

#### 4.3.4 Turning Performance

An important aspect of successfully completing all of the missions is the ability of the aircraft to turn quickly and tightly. It was determined that a maximum load factor of 1.5g was acceptable to ensure the structural integrity of the aircraft. The maximum rotation rate can be calculated by Equation 12, where  $n_{zs}$  is the load factor.

$$\Omega_{\max} = \frac{g}{V_{\text{stall}}} \sqrt{n_{zs} - \frac{1}{n_{zs}}} \quad (12)$$

This yields a maximum rotation rate of 33.80 deg/s for the empty aircraft. Over the course of a lap, the aircraft will be required to turn 720 degrees, leading to a total turning time of approximately 21 seconds. From the maximum rotation rate the minimum turning radius can be calculated by Equation 13.

$$\frac{1}{R_{\min}} = \frac{\Omega_{\max}}{\sqrt{n_{zs} V_{stall}}} \quad (13)$$

As such, the minimum turning radius for the empty aircraft is 64.63 feet. This is quite small compared to the approximately 1,000.00 foot length of the competition pattern, allowing the aircraft to efficiently turn around without substantially increasing the distance flown.

#### 4.3.5 Uncertainty Analysis

Any theoretical analysis of aircraft flight characteristics necessarily includes a number of assumptions and simplifications. There are factors that will affect the aircraft in flight that were not included in the analysis, including the presence of the fuselage and weather conditions. In order to determine the handling qualities of the aircraft both as well as its performance in adverse weather conditions, a variety of flight tests are required. An important weather consideration is the frequency of high winds at the competition site in Wichita, Kansas. Although flight testing is required to confirm the analysis, the team is confident that the analysis produced accurate general characteristics, showing the workability of the design.

## 5 Detailed Design

The following section describes the finalized design of Ursa Major in detail from a subsystem level and includes a center of gravity analysis, aircraft performance, mission performance, and a CAD drawing package.

### 5.1 Subsystem Design

#### 5.1.1 Wing Detailed Design

The configuration for the wing is a tapered high-wing with no dihedral and flaperon control surfaces. The high-wing design supports short takeoff distances, eases manual cargo loading, and allows the wing to swivel. The high-wing design increases the stability of the aircraft, eliminating the need for a dihedral angle. The wing is tapered to save weight and increase the aspect ratio for the set wingspan and area as per the limited maximum takeoff distance and wingspan.

Because of the short takeoff requirement, flaperons were implemented, increasing the lifting capabilities of the wing at lower velocities while simultaneously increasing maneuverability. Detailed dimensions are located in Table 5.1.1, as calculated by the sizing script. The CAD design for the wood and carbon fiber pieces of the wing were modeled in SOLIDWORKS, as shown in Figures 5.1.1, 5.1.2, 5.1.3. Additional stringers were attached to the ribs to provide structure and attachment points for the MonoKote. One carbon fiber spar, running through both wings, provides structural support and a method of integration for the wings into the swivel piece. There is one servo contained in a plate on the lower surface of each wing. Control rods extend the servo motion to each flaperon. Hinge points connect the flaperons to the main wing.

The team investigated developed an experimental control surface structure for the wing, which mainly consisted of a 0.25 inch square basswood dowel inserted through the ailerons and flaps. This rod is connected to both wing tips, acting as the main rotation point for the control surfaces. In addition, this design also introduced polystyrene foam pieces at the front of the ailerons and flaps, helping to narrow the gap between the control surface and the wing.

Parameter	Value
Airfoil	NACA 6515
Planform Area (in <sup>2</sup> )	771.04
Aspect ratio	4.40
Wingspan (in)	58.00
Root chord (in)	14.60
Tip chord (in)	11.67
Taper ratio	0.80
Flaperon chord percentage	25%
Aileron wingspan percentage	80%
Estimated mass (lbs)	0.418

Table 5.1.1: Wing Dimensions

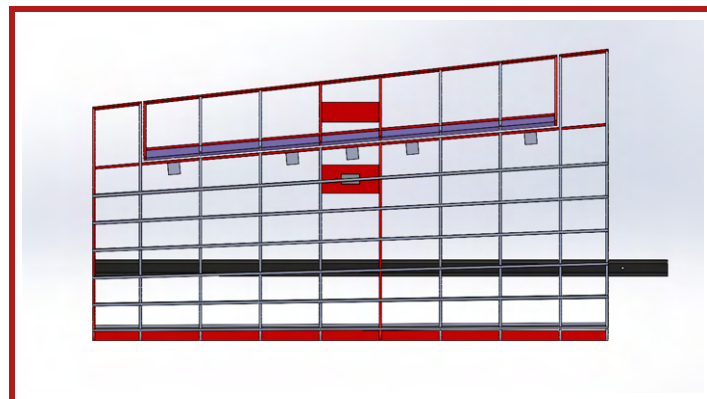


Figure 5.1.1: Top View

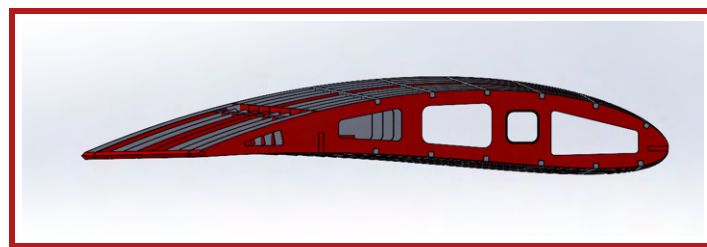


Figure 5.1.2: Tip View

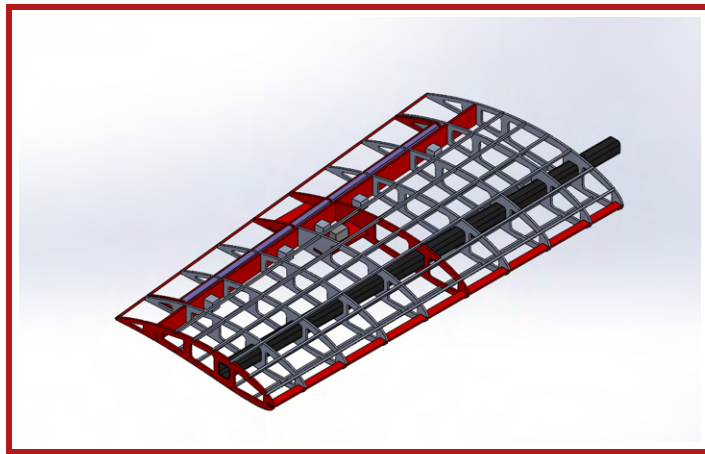


Figure 5.1.3: Isometric View

### 5.1.2 Wing Integration Detailed Design

A swiveling wing design was chosen to allow the flight configuration's five-foot wingspan to rotate into the parking configuration's 2.50-foot wingspan requirement. To accomplish this, the wing box connecting the wing to the fuselage (Figure 5.1.4) requires the wing to rotate around the vertical axis. The team accomplished this by constructing the wing box out of two 3D-printed Onyx integration pieces. The wing spar is inserted through one piece, and is fixed in place with nuts and bolts, while the fuselage spar is inserted through the other. Subsequently, they are joined around a ball bearing with a one-inch outer radius and 0.50-inch height. This allows the two pieces to rotate up to 90 degrees relative to each other. The component into which the ball bearing is inserted has a 1.00-inch radius, with a 0.005-inch tolerance, which created sufficient friction to ensure that the two components remained in parking configuration.

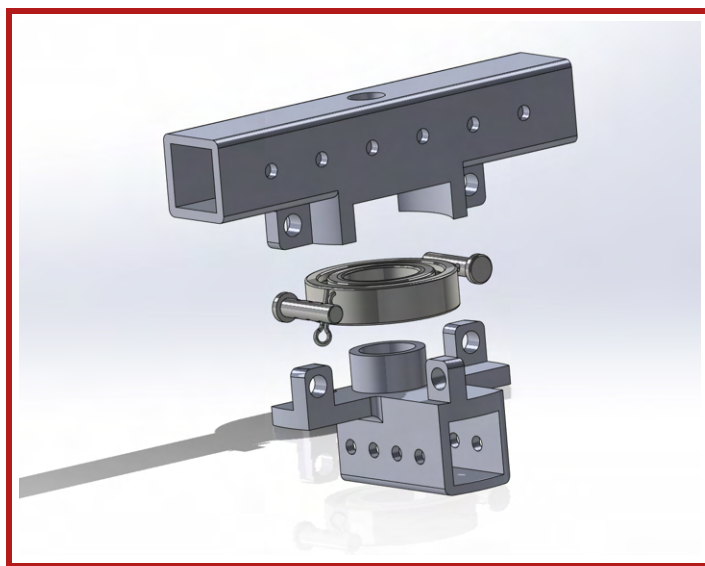


Figure 5.1.4: Exploded View of the Wing Box

To increase security in flight, the two integration pieces are also held together with a pair of clevis pins. This mechanism prevents the wing from rotating while midair. The top integration piece rotates about the vertical axis until

it collides with the extruded parts of the bottom integration piece. In the parking configuration, the wing is parallel to the fuselage, allowing it to easily fit into the parking space. To switch into flight configuration, the integration piece rotates the maximum angle of 90 degrees until the pieces are lined up, at which point clevis pins and cotter pins would be inserted to lock rotation.

A large amount of drag would be induced by the wing box due to its angular design. Therefore, a cover that matches the contour of the airfoil was designed to fit over the integration piece to achieve a more streamlined aerodynamic flow (Figure 5.1.5). The cover was constructed of lightweight foam and secured with Velcro straps attached to the fuselage ahead of and behind the airfoil.

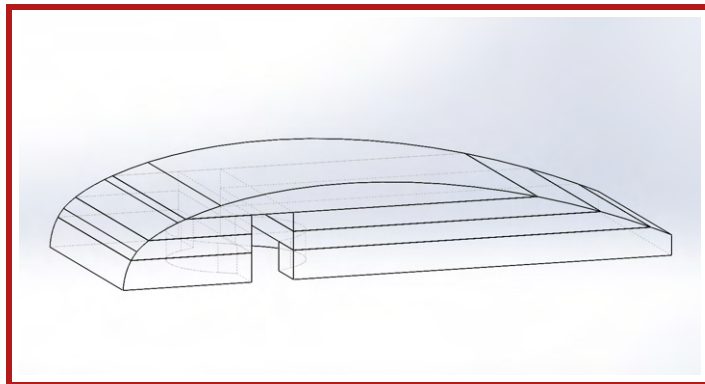


Figure 5.1.5: Aerodynamic Foam Cover

### 5.1.3 Empennage Detailed Design

The dimensions of both the stabilizers were determined during sizing and scoring analysis. Neither stabilizer will have any taper because the team decided that any benefit towards drag would not outweigh the effects of changing the area of the control surfaces. Table 5.1.2 summarizes the geometric parameters that were used when creating the empennage.

Parameter	Horizontal Stabilizer	Vertical Stabilizer
Airfoil	NACA 0012	NACA 0012
Tail lever arm (in)	38.00	38.00
Planform Area (in <sup>2</sup> )	187.57	67.33
Aspect Ratio	2.48	1.88
Span (in)	21.56	11.24
Chord (in)	8.70	5.99

Table 5.1.2: Summary of Empennage Geometric Parameters

The widths of the airfoil ribs for both the vertical and horizontal stabilizers are 1/8 inch to balance structural strength, structural weight, and ease of manufacturing. The length of the tail arm was chosen to give an adequate moment arm for the aircraft pitching. This allows the control surfaces to create a large enough moment about the center of mass so that the plane would be well-controlled during flight.

For the control surfaces, the team decided to have a 35.50% elevator chord and a 43.20% rudder chord. The trailing edges of the control surfaces are balsa pieces. The elevator is a single piece that extends the entirety of the horizontal stabilizer to create a more consistent elevator movement and to simplify the rotating mechanism and

improve takeoff capabilities. Similar to the wing, polystyrene foam pieces were added to the outside faces of the leading comb of the control surfaces to aid in aerodynamic efficiency. In addition to the foam pieces, wooden balsa blocks were also placed on the inner faces of the rear comb of the stabilizers to give the hinge pins a depth to hold onto, intending to reduce the gap between the stabilizer and control surface, and to keep the hinge pins from shifting around during flight.

Due to the T-tail having most of its weight centered above the tail integration piece, there are two support structures each for both the vertical and horizontal stabilizers to stabilize the empennage. These are placed at opposing ends of the static section of the vertical stabilizer to ensure that this part is secure.

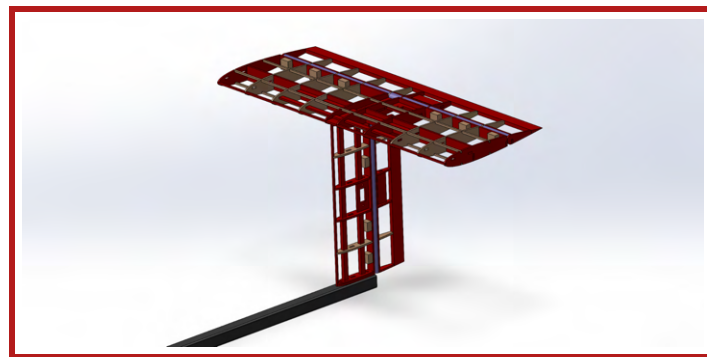


Figure 5.1.6: Empennage Detailed Design

#### 5.1.4 Empennage Integration Detailed Design

The integration of the empennage onto the main spar was achieved by attaching the vertical stabilizer onto the main spar with a screw positioned at either end of the vertical stabilizer. The bottom rib of the vertical stabilizer lays flat on the top of the main spar with two ribs stacked on top of each other to strengthen the integration. The vertical stabilizer hardwood spars also meet the lower surface of the bottom rib. Holes were drilled through the two bottom ribs and the main spar for the screws, where they were fastened with nuts.

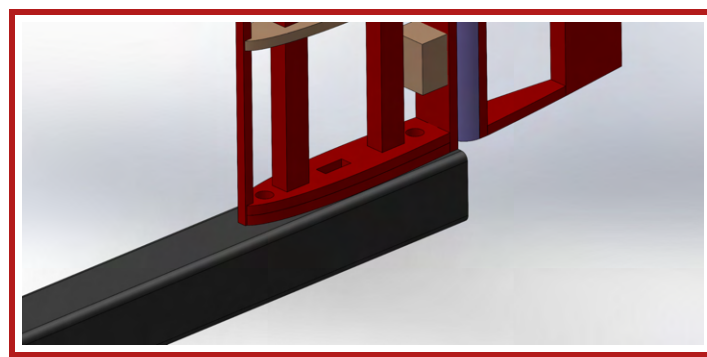


Figure 5.1.7: Empennage Integration Detailed Design

### 5.1.5 Fuselage Detailed Design

The aircraft fuselage is designed to optimize weight, cost, and cargo capacity without sacrificing structural integrity. The semi-monocoque structure consists of a series of wooden ribs attached to a carbon fiber spar passing through the top of the ribs. Ribs at the front and rear, as well as ribs supporting the wing, are made from basswood since they bear more of the loads in flight. The remaining ribs are made from balsa to save weight. The ribs of the main structure have a rectangular cutout to maximize cargo space for mission components. These cutouts also save weight and allow wires to be routed through the fuselage. The bottom of the front ribs were removed to accommodate the electronics package. The nose cone section consists of a 3D-printed Onyx component and crew hatch to make the aircraft more aerodynamic and accommodate the pilots, respectively. The crew hatch and side hatch will be attached to the fuselage with metal hinges. On the left of the fuselage, the ribs were modified to allow for a swing hatch.

Thin wooden stringers were slotted and glued into notches cut into the sides of the ribs. These stringers give the fuselage form, and give support to the MonoKote wrapped over the fuselage to improve aerodynamics. Inside of the fuselage, a basswood base plate supports the mission components. Figure 5.1.8 depicts the CAD rendering of the fuselage.

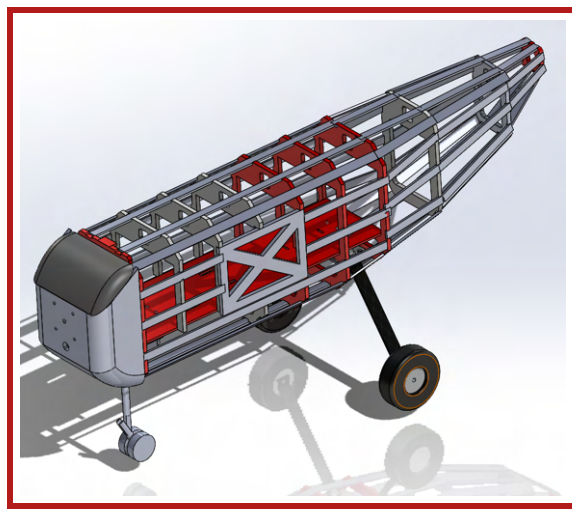


Figure 5.1.8: Full Fuselage CAD; Red represents basswood, gray represents balsa.

The nose cone was designed to optimize weight and structural strength. It consists of an Onyx 3D-printed component with two platforms for the Crew, six wedges for fuselage integration, and the motor mount section on the front. Whereas a solid design would be the most structurally sound, weight was an important factor close to the front of the plane, especially due to the already heavy weight of the motor and propeller. Therefore, a hollowed-out design was chosen to minimize the weight while maintaining a structural outline and frame. The strength of the material will enable the frame to support the motor along with the crew. Additional wedges were built into the frame to act as locations for screws mounting the nose cone to the rest of the fuselage. These have been positioned in the four outer corners, with two more supporting the middle just under the motor. This enables the nose cone to attach securely to the fuselage. To integrate the nose cone with the fuselage, 3/16 inch stainless steel machined screws screw from the fuselage bulkhead into the integration screw holes on the nose cone. These screws were chosen due to their low weight and strong securing abilities. Figure 5.1.9 depicts a detailed view of the interior and exterior of the nose cone.

The fuselage length is 33.40 inches from the nose cone to the rearmost rib. The width is 6.00 inches and height is 8.00 inches. The cargo hold is 17.00 inches x 5.00 inches x 3.90 inches, with a cargo capacity of 331.50 cubic

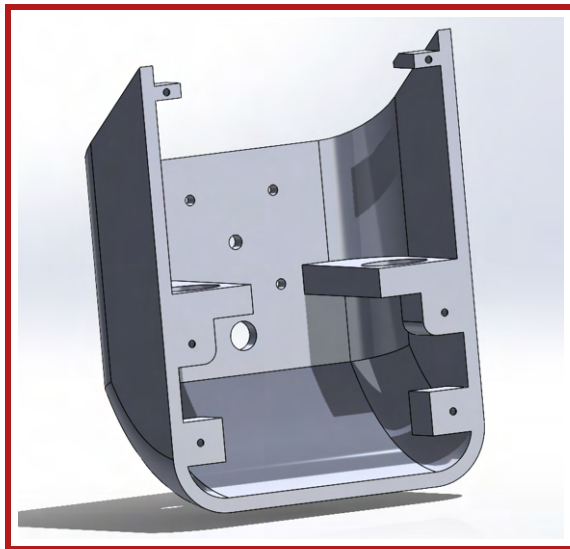


Figure 5.1.9: Nose Cone CAD

inches. The ribs, base plate, and stringers are 1/8 inches thick, with the stringer width being 1/2 inch. Nose cone dimensions are 6.00 inches x 7.70 inches x 3.00 inches, the crew hatch dimensions are 6.00 inches x 3.60 inches x 0.90 inches, and the side hatch dimensions are 6.00 inches x 4.30 inches x 0.13 inches.

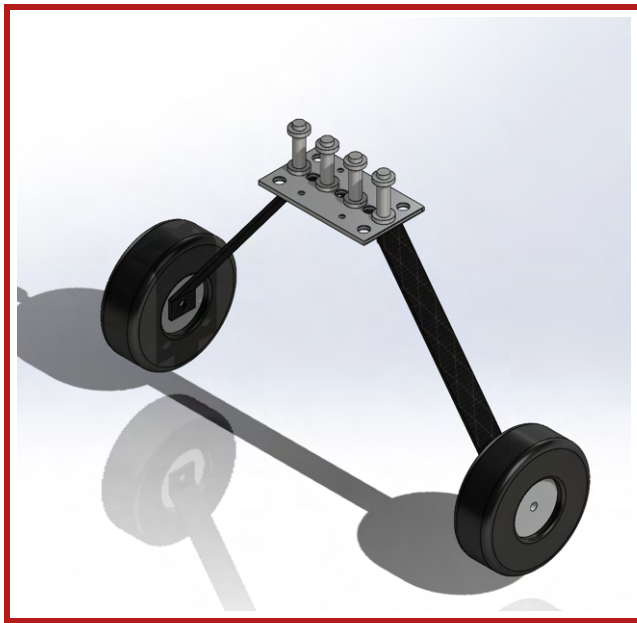
### 5.1.6 Landing Gear Detailed Design

The main landing gear is made predominantly of a carbon fiber frame which minimizes the main gear's weight and improve its strength. Lightweight foam wheels are attached to the bottom of the frame. To allow clearance for the 13.00 inch propeller, the landing gear raises the plane approximately 9.00 inches off the ground allowing for 2.50 inches of propeller clearance. A 3D-printed PLA integration piece that endures high stress and aids in absorbing the landing forces are attached to the top of the carbon fiber frame. The main gear is attached to the fuselage with 0.25 inch diameter, 2.00 inch bolts and 0.25 inch lock nuts that secure it to a wood base plate. 0.25 inch washers and circular felt pads placed in between the fasteners and the base plate in order to distribute force. For maximum stability, the main gear is placed at between a 6.00 and 20.00 degree angle from the vertical, behind the center of mass [12], in between the fourth and fifth ribs of the fuselage. Figure 5.1.10 depicts a CAD rendering of the main landing gear along with how it is integrated with the fuselage.

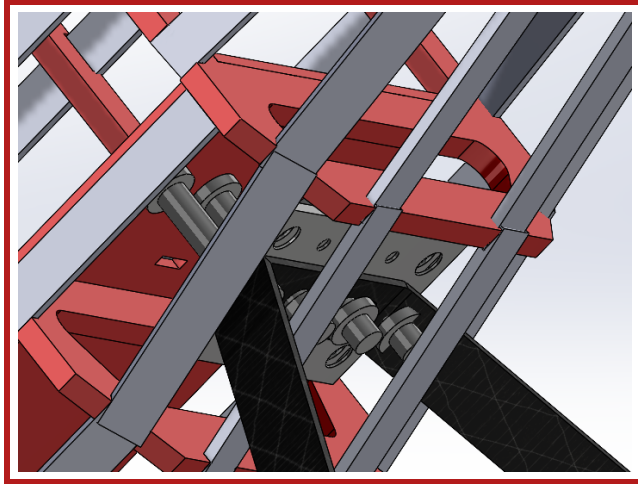
The nose gear is placed at the leading edge of the fuselage. It is mounted on the front rib of the fuselage with a servo to enable steering capabilities. It is made with two wheels and springs to aid in absorbing some of the landing/takeoff forces. The nose gear is located 40 degrees from the vertical of the center of mass, towards the front of the plane. It is secured to the fuselage with 0.25 inch diameter, 2.50 inch bolts and nuts to add more space for the servo to function without interference. These landing gear characteristics allow it to support the aircraft while prioritizing stability, weight, and durability. Figure 5.1.11 depicts a CAD rendering of the nose gear.

### 5.1.7 Mission Package Detailed Design

**Mission 2** To integrate the MSC, the gurney, the EMT's, the Crew and the Patient, a baseplate of dimensions 9.00 inches x 3.41 inches with notches is used for M2. Notches were used to aid in the insertion of the M2 package and



(a) Main Landing Gear with Integration Piece



(b) Main Gear Integration into Fuselage

Figure 5.1.10: Main Landing Gear With Integration

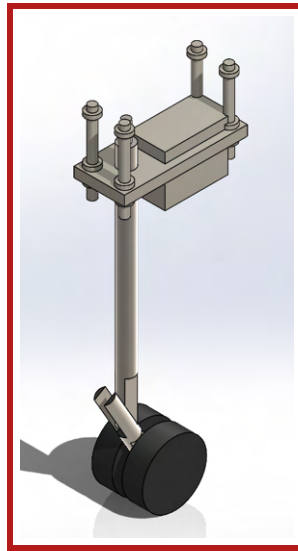


Figure 5.1.11: Nose Landing Gear

hold it in place. Following the AIAA competition rules, the MSC needed minimum dimensions of 3.00 inches x 3.00 inches x 3.50 inches. The MSC and gurney were 3D-printed using ABS material to ensure it was lightweight, strong, and met tolerancing requirements to securely hold the Patient. The EMTs are positioned next to the Patient using a rectangular base with two extruded circular holes that were cut to fit the base of the EMTs securely. This base has two rectangular notches at its base, which slot into holes in the fuselage. To ensure stability, the EMT restraint is also secured to the fuselage with Velcro. Figure 5.1.12 depicts the CAD renderings of the various printed components that make up M2.

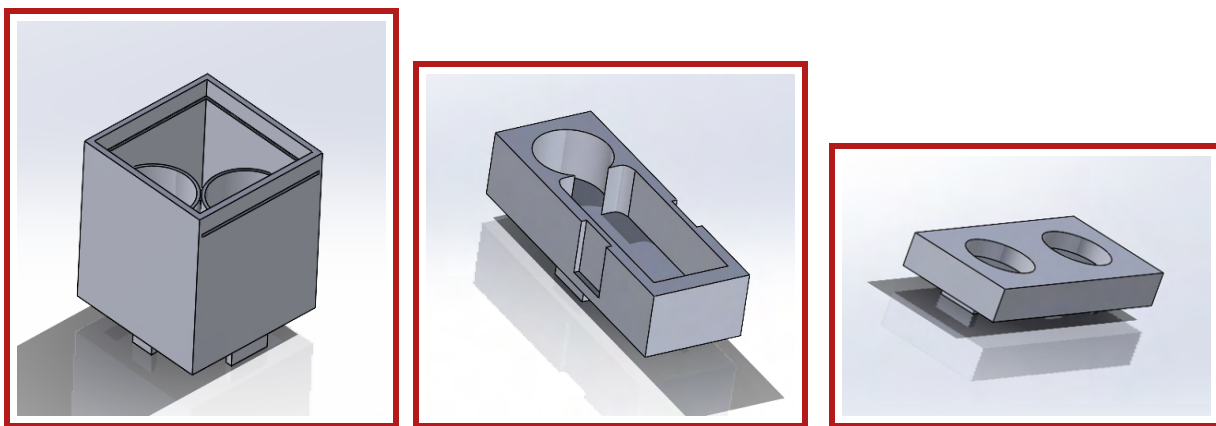


Figure 5.1.12: Side by side view of the components that make up M2 in SOLIDWORKS

**Mission 3** For M3 the space inside of the fuselage was optimized to carry as many Passengers as possible. At the same time, the passenger integration baseplate must be easy to quickly maneuver into place as well as remove from the fuselage. To ensure efficient transitions between mission configurations for the GM, the passenger integration base plate was split into three sections which were connected with a hook and notch attachment that slid into place. While splitting the base plate into three sections lowers the total number of Passengers that will be able to fit in the fuselage, the increased maneuverability was deemed more favorable than the potential extra Passengers loaded. This design provides space for 33 Passengers. Each section is 5.82 inches x 5.00 inches x 0.25 inches, 5.86 inches x 5.00 inches x 0.25 inches, and 5.82 inches x 5.00 inches x 0.25 inches. As with M2, 3D printing ensures precise sizing of passenger slots, so the Passengers will fit inside and not fall out during the flight. Figures 5.1.13 and 5.1.14 depict the various passenger inserts and the assembled insert configuration.

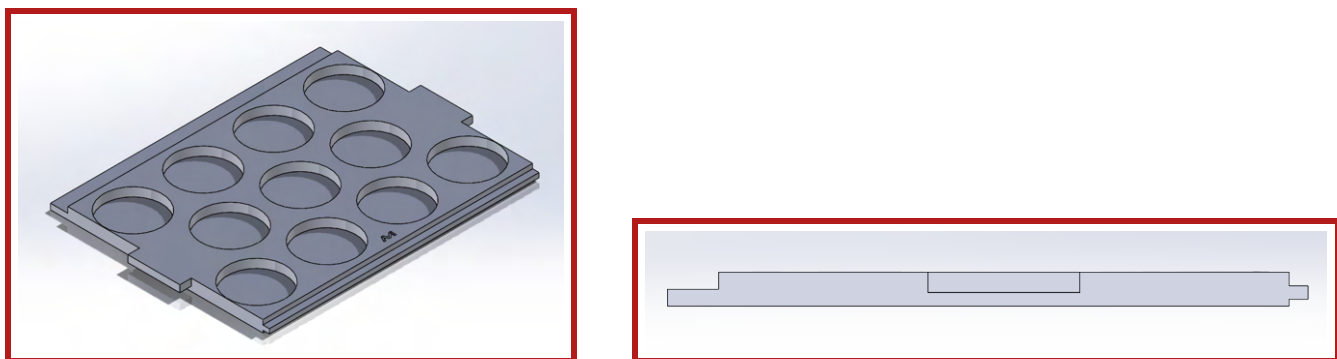


Figure 5.1.13: CAD of the middle insert for passengers and a side view showing the notch layout.

For restraints, two methods were combined to ensure as much stability during flight as possible. These methods are a wooden lattice structure (placed over the passengers) and adhesive rubber backings (placed inside the passenger cutouts). These ensure compliance with rules and consistent spacing between Passengers and makes GM easier to complete within the time limit. The wooden lattice structure was laser cut from balsa wood and the design was taken directly from the CAD of the insert, to ensure the layout of the holes is exact. The adhesive rubber was purchased from Amazon and was cut into small strips, which were placed inside the cutouts to provide extra grip and prevent sliding.

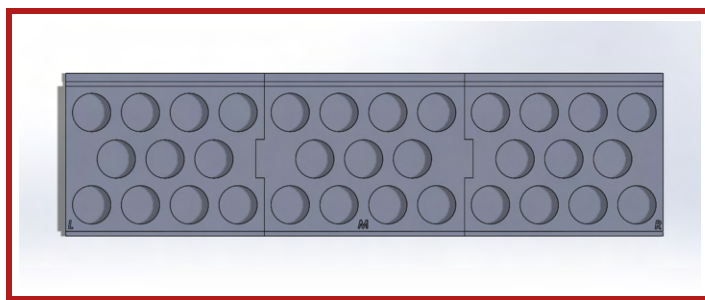


Figure 5.1.14: CAD showing the inserts press fit together, as they will be inside the fuselage.

### 5.1.8 Propulsion Detailed Design

A single ManiaX 6s 2400mAh lithium-polymer battery provides power to the propulsion system necessary to sustain flight for all three flight missions. A single tractor propulsion system serves as the propulsion configuration, consisting of a Cobra C-4120/22 motor paired with an APC 15x8 propeller to provide thrust to the aircraft. An external arming plug is also mounted to satisfy AVIO 5. Table 5.1.3 depicts the major components used for the propulsion system. This system is used for all three flight missions.

Component	Details
Battery	ManiaX 2400mAh 6s 80C LiPo
ESC	Cobra 60A ESC
Motor	Cobra C-4120/22 430Kv Brushless Motor
Propeller	15x8 APC Propeller

Table 5.1.3: Final Propulsion System Configuration

In addition, all control surfaces are actuated by EcoPower 640T servos that are connected to a Spektrum 8-channel receiver and is controlled by a Spektrum DX-8e transmitter. The receiver itself is separate from the propulsion system, thus a separate NiMH battery fitted with an external switch is used to power the receiver (AVIO 5). Figure 5.1.15 depicts the wiring diagram of the aircraft.

### 5.1.9 Electronics Integration Detailed Design

The electronics integration piece is designed to organize the wires and electronics within the fuselage. The piece is a 3D-printed block containing slots for all of the electronic components within the fuselage, which is Velcroed onto the fuselage. It extends the plane for easy access between missions. The hatch hinge is on the side of the underbelly of the fuselage to allow for a larger range of motion. The hatch also extends up the side of the fuselage to the top of the base plate, allowing for increased visibility of the stored components. (Shown in 5.1.16)

The integration piece is attached upside-down to the bottom of the hardwood base plate to minimize strain on the hatch. Four holes were added to secure the structure with nuts, as well as Velcro straps to attach the electrical components firmly. The weight was reduced by minimizing the side supports. To evenly distribute the mass, the team placed the battery as close to the center of gravity as possible. The integration piece wraps around the space constraining the front landing gear, leaving the battery directly behind it and the lighter components on the outer edges. Making space for the landing gear, the final dimensions of the piece are 4.22 x 8.25 x 1.10 inches. Accounting for possible mid-flight torque, the team added extra length to the latch mechanism to decrease the risk of mechanical

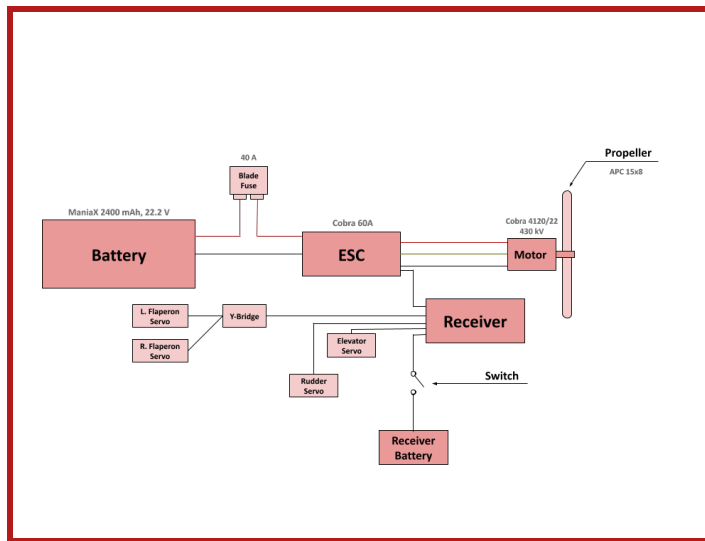


Figure 5.1.15: Diagram of Electronics System

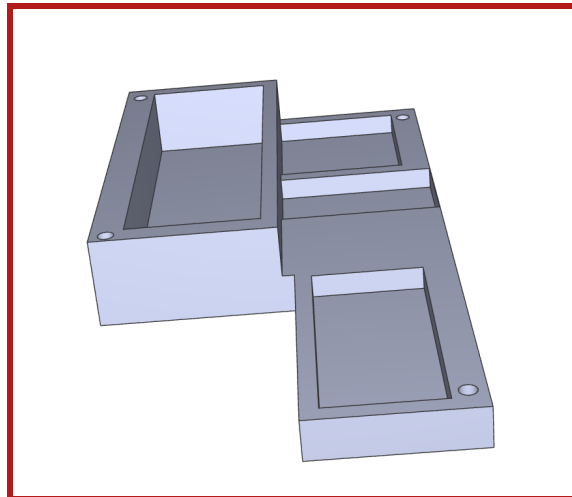


Figure 5.1.16: Electronics Integration Piece

failure. An L-shaped pin runs through the inside of the latch and turns to lock the hatch closed by sliding in place in the fuselage. The bottom of the latch contains an exposed turning pin, which can be rotated with a flathead screwdriver. This design offers the least amount of drag to the underside of the plane, as the screwdriver's head permits access even when the screw is flush with the plane. The team elected to use two latches, instead of one, to better distribute the load of the integration piece along the fuselage.

### 5.1.10 Motor Integration Detailed Design

Due to the left-turning tendency commonly exhibited by RC aircraft, the motor is angled slightly to the right to account for the P-factor. A standard thrust angle of 2.00 degrees was selected following market research on standard RC plane practices [13]. The distance between motor mount holes on Ursa Major is 1.22 inches. The motor angle height, or the height the motor must be raised on one side to achieve the selected thrust angle, can be calculated using

Equation 14.

$$\text{Motor Angle Height} = \text{Distance Between Motor Mount Holes} \times \tan(\text{Thrust Angle}) \quad (14)$$

The team calculated the motor angle height to be 0.04 inches. To achieve this, the team stacked spacers to the calculated height under the left side of the motor mount. The motor offset, or the amount of space the motor must be moved to the right on the nose cone is calculated using Equation 15. As such, the motor is offset to the right by 0.09 inches to counter the P-factor.

$$\text{Motor Offset Distance} = \text{Engine Length} \times \sin(\text{Thrust Angle}) \quad (15)$$

## 5.2 Weight and Balance

The positioning of certain loads, and consequently the total mass of the aircraft, changes between each mission. Following these changes, calculations were performed to determine the optimal center of gravity for aircraft performance. Table 5.2.1 summarizes the center of mass of all the major components on Ursu Major. The center of mass of each component was determined using SOLIDWORKS, with reference to the center of gravity of the M1 configuration; that is, the positive x-axis points towards the nose of the aircraft, the positive y-axis points towards the right wing, and the positive z-axis points towards the ground.

Component	Mass (lbs)	CGx (in)	CGy (in)	CGz (in)
<b>All Missions</b>				
Fuselage	3.53	-1.11	0.00	3.25
Main Landing Gear	0.32	-6.22	0.00	9.98
Nose Gear	0.20	8.03	0.00	8.28
Wing	0.78	0.55	0.00	-2.45
Tail	0.55	-24.27	0.00	-7.13
Motor	0.85	13.98	0.00	2.28
Propeller	0.019	15.50	0.00	2.28
Esc	0.025	5.95	1.00	4.64
<b>Mission 1</b>				
Battery	0.791	5.95	-0.43	4.64
<b>Total</b>	<b>6.61</b>	<b>0.00</b>	<b>0.00</b>	<b>0.00</b>
<b>Mission 2</b>				
Battery	0.79	5.95	-0.43	4.64
EMTs	0.15	1.74	1.55	3.60
Patient + Gurney	0.56	1.74	0.50	3.44
Medical Supply Cabinet	1.44	-4.01	0.00	2.72
<b>Total</b>	<b>9.65</b>	<b>-1.01</b>	<b>0.09</b>	<b>1.45</b>
<b>Mission 3</b>				
Battery	0.74	5.95	-0.43	4.64
Inserts	0.45	-0.26	0.00	-4.19
Passengers	2.02	-0.26	0.00	-3.60
<b>Total</b>	<b>8.94</b>	<b>-0.11</b>	<b>0.00</b>	<b>1.26</b>

Table 5.2.1: Weight and Balance for Ursu Major

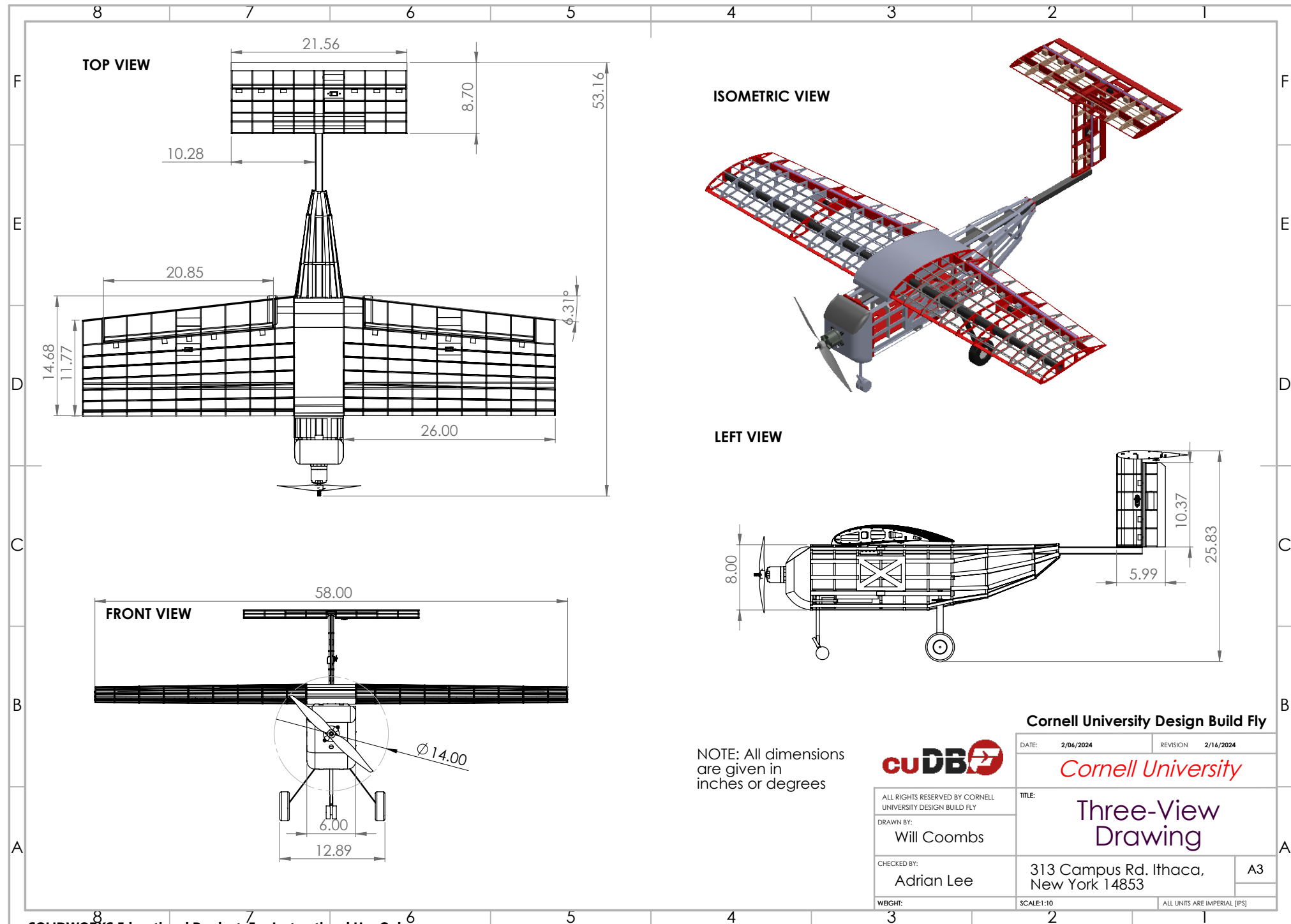
### 5.3 Aircraft Performance

As the detailed design is derived from the preliminary design, the expected aerodynamics performance and mission performance has not changed. XFLR5 serves as the team's primary software to run lift, drag, and static and dynamic stability simulations. From there, the team is able to estimate mission flight speeds and flight times. Sections 4.3.2 and 4.3.3 explain these performance calculations in detail. Table 5.3.1 summarizes the expected aircraft performance parameters.

Parameter	M1	M2	M3
Mass (lb)	7.85	10.49	8.99
$C_{L,cruise}$	0.43	0.46	0.46
$C_{D,cruise}$	0.03	0.03	0.03
$C_L/C_{Dcruise}$	14.33	15.33	15.33
$V_{cruise}$ (feet/s)	53.6	59.38	54.99

Table 5.3.1: Expected Aerodynamic and Mission Performance

### 5.4 Drawing Package



Cornell University Design Build Fly



Cornell University

ALL RIGHTS RESERVED BY CORNELL UNIVERSITY DESIGN BUILD FLY

DRAWN BY:  
Will Coombs

CHECKED BY:  
Adrian Lee

DATE: 2/06/2024 REVISION 2/16/2024

TITLE: Three-View Drawing

313 Campus Rd. Ithaca, New York 14853

SCALE: 1:10 ALL UNITS ARE IMPERIAL [IPS]

	8	7	6	5	4	3	2	1																																																																																																																
F								F																																																																																																																
E								E																																																																																																																
D								D																																																																																																																
C								C																																																																																																																
B								B																																																																																																																
A								A																																																																																																																
<p>NOTE: All dimensions are given in inches or degrees</p> <p><b>DETAIL A</b> SCALE 1 : 4</p> <p><b>DETAIL B</b> SCALE 1 : 4</p>																																																																																																																								
<table border="1" style="width: 100%; border-collapse: collapse;"> <thead> <tr> <th>ITEM NO.</th> <th>PART NUMBER</th> <th>Material/Product</th> <th>QTY.</th> </tr> </thead> <tbody> <tr><td>1</td><td>Motor</td><td>Cobra C-4120/22</td><td>1</td></tr> <tr><td>2</td><td>Propeller</td><td>APC</td><td>1</td></tr> <tr><td>3</td><td>Motor Mount</td><td>Aluminum</td><td>1</td></tr> <tr><td>4</td><td>Nose Cone</td><td>ABS</td><td>1</td></tr> <tr><td>5</td><td>Nose Hatch</td><td>ABS</td><td>1</td></tr> <tr><td>6</td><td>Swivel Wing Integration Piece</td><td>Onyx (CF Fiber)</td><td>1</td></tr> <tr><td>7</td><td>Fuselage Swivel Integration Piece</td><td>Onyx</td><td>1</td></tr> <tr><td>8</td><td>Wing Cover</td><td>Foam</td><td>1</td></tr> <tr><td>9</td><td>Fuselage Hatch</td><td>Balsa</td><td>1</td></tr> <tr><td>10</td><td>Nose Gear</td><td>Aluminum</td><td>1</td></tr> <tr><td>11</td><td>Nose Wheel</td><td>Foam</td><td>1</td></tr> <tr><td>12</td><td>Wing Spar</td><td>Carbon Fiber</td><td>1</td></tr> <tr><td>13</td><td>Wing</td><td>Basswood/Balsa</td><td>1</td></tr> <tr><td>14</td><td>Flaperon</td><td>Basswood/Balsa</td><td>2</td></tr> <tr><td>15</td><td>Fuselage</td><td>Basswood/Balsa</td><td>1</td></tr> <tr><td>16</td><td>Fuselage Baseplate</td><td>Basswood</td><td>1</td></tr> <tr><td>17</td><td>Horizontal Stabilizer</td><td>Basswood/Balsa</td><td>1</td></tr> <tr><td>18</td><td>Elevator</td><td>Basswood/Balsa</td><td>1</td></tr> <tr><td>19</td><td>Vertical Stabilizer</td><td>Basswood/Balsa</td><td>1</td></tr> <tr><td>20</td><td>Rudder</td><td>Basswood/Balsa</td><td>1</td></tr> <tr><td>21</td><td>Tail Spar</td><td>Carbon Fiber</td><td>1</td></tr> <tr><td>22</td><td>Servo</td><td>EcoPower 640T</td><td>4</td></tr> <tr><td>23</td><td>Landing Gear Baseplate</td><td>Basswood</td><td>1</td></tr> <tr><td>24</td><td>Main Landing Gear</td><td>Carbon Fiber</td><td>1</td></tr> <tr><td>25</td><td>Main Wheels</td><td>Foam</td><td>2</td></tr> <tr><td>26</td><td>Electronics Integration Piece</td><td>ABS</td><td>1</td></tr> <tr><td>27</td><td>Hinge</td><td>Plastic</td><td>19</td></tr> </tbody> </table>									ITEM NO.	PART NUMBER	Material/Product	QTY.	1	Motor	Cobra C-4120/22	1	2	Propeller	APC	1	3	Motor Mount	Aluminum	1	4	Nose Cone	ABS	1	5	Nose Hatch	ABS	1	6	Swivel Wing Integration Piece	Onyx (CF Fiber)	1	7	Fuselage Swivel Integration Piece	Onyx	1	8	Wing Cover	Foam	1	9	Fuselage Hatch	Balsa	1	10	Nose Gear	Aluminum	1	11	Nose Wheel	Foam	1	12	Wing Spar	Carbon Fiber	1	13	Wing	Basswood/Balsa	1	14	Flaperon	Basswood/Balsa	2	15	Fuselage	Basswood/Balsa	1	16	Fuselage Baseplate	Basswood	1	17	Horizontal Stabilizer	Basswood/Balsa	1	18	Elevator	Basswood/Balsa	1	19	Vertical Stabilizer	Basswood/Balsa	1	20	Rudder	Basswood/Balsa	1	21	Tail Spar	Carbon Fiber	1	22	Servo	EcoPower 640T	4	23	Landing Gear Baseplate	Basswood	1	24	Main Landing Gear	Carbon Fiber	1	25	Main Wheels	Foam	2	26	Electronics Integration Piece	ABS	1	27	Hinge	Plastic	19
ITEM NO.	PART NUMBER	Material/Product	QTY.																																																																																																																					
1	Motor	Cobra C-4120/22	1																																																																																																																					
2	Propeller	APC	1																																																																																																																					
3	Motor Mount	Aluminum	1																																																																																																																					
4	Nose Cone	ABS	1																																																																																																																					
5	Nose Hatch	ABS	1																																																																																																																					
6	Swivel Wing Integration Piece	Onyx (CF Fiber)	1																																																																																																																					
7	Fuselage Swivel Integration Piece	Onyx	1																																																																																																																					
8	Wing Cover	Foam	1																																																																																																																					
9	Fuselage Hatch	Balsa	1																																																																																																																					
10	Nose Gear	Aluminum	1																																																																																																																					
11	Nose Wheel	Foam	1																																																																																																																					
12	Wing Spar	Carbon Fiber	1																																																																																																																					
13	Wing	Basswood/Balsa	1																																																																																																																					
14	Flaperon	Basswood/Balsa	2																																																																																																																					
15	Fuselage	Basswood/Balsa	1																																																																																																																					
16	Fuselage Baseplate	Basswood	1																																																																																																																					
17	Horizontal Stabilizer	Basswood/Balsa	1																																																																																																																					
18	Elevator	Basswood/Balsa	1																																																																																																																					
19	Vertical Stabilizer	Basswood/Balsa	1																																																																																																																					
20	Rudder	Basswood/Balsa	1																																																																																																																					
21	Tail Spar	Carbon Fiber	1																																																																																																																					
22	Servo	EcoPower 640T	4																																																																																																																					
23	Landing Gear Baseplate	Basswood	1																																																																																																																					
24	Main Landing Gear	Carbon Fiber	1																																																																																																																					
25	Main Wheels	Foam	2																																																																																																																					
26	Electronics Integration Piece	ABS	1																																																																																																																					
27	Hinge	Plastic	19																																																																																																																					

Cornell University Design Build Fly



DATE: 2/1/2024 REVISION 2/4/2024

Cornell University

## Structural Arrangement

ALL RIGHTS RESERVED BY CORNELL UNIVERSITY DESIGN BUILD FLY	TITLE:
DRAWN BY: Will Coombs	
CHECKED BY: Adrian Lee	313 Campus Rd. Ithaca, New York 14853
WEIGHT: 6.61 pounds	SCALE: 1:8
	ALL UNITS ARE IMPERIAL [IPS]

8

7

6

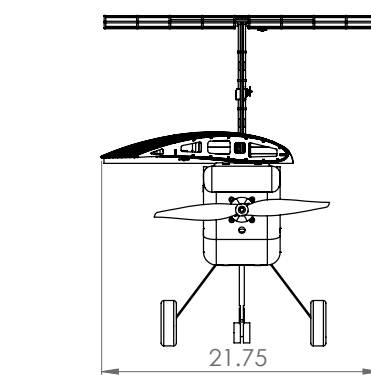
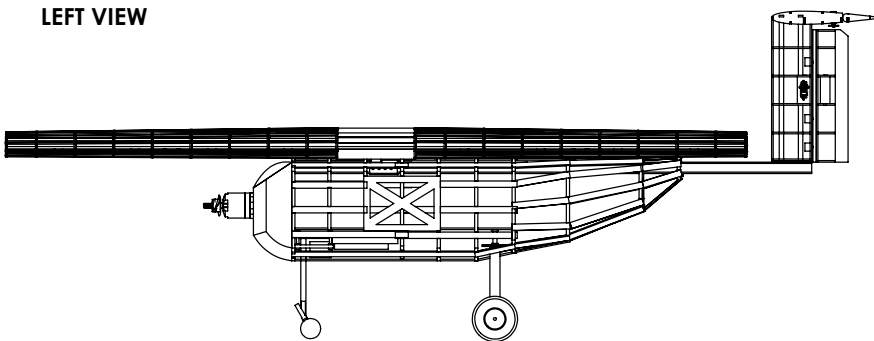
5

4

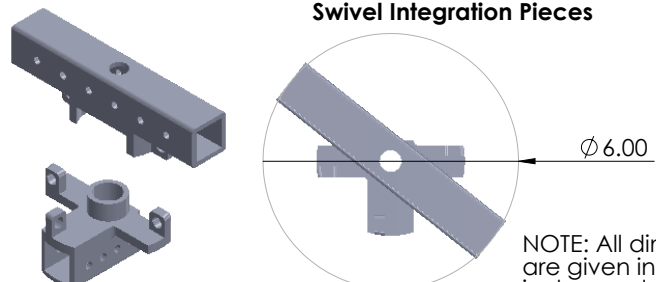
3

2

1

**FRONT VIEW****ISOMETRIC VIEW****Parking Configuration****LEFT VIEW**

Scale 1:3

**Swivel Integration Pieces**

NOTE: All dimensions  
are given in  
inches or degrees

68.55

F

E

D

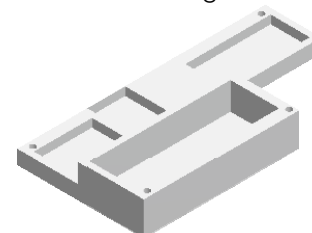
C

B

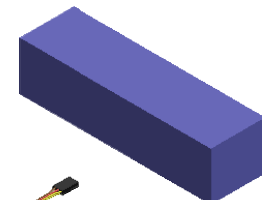
A

**Electronics Systems**

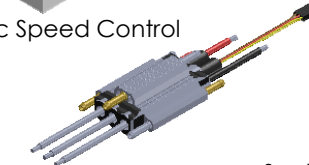
Electronics Integration Piece



80C Lipo Battery



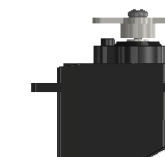
Electronic Speed Control



Scale 1:3

**Electronics Systems**

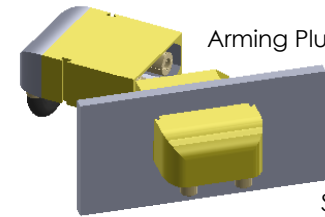
ECP-640T Servo



AR7000 Reciever



Arming Plug



Scale 1:1

Cornell University Design Build Fly



DATE: 2/6/2024 REVISION 2/9/2024

Cornell University

TITLE:  
**Systems Layout/  
Parking Configuration**

ALL RIGHTS RESERVED BY CORNELL  
UNIVERSITY DESIGN BUILD FLY

DRAWN BY:

Will Coombs

CHECKED BY:

Adrian Lee

WEIGHT: 6.61 pounds

SCALE: 1:10

313 Campus Rd. Ithaca,  
New York 14853

A3

ALL UNITS ARE IMPERIAL [IPS]

8

7

6

5

4

3

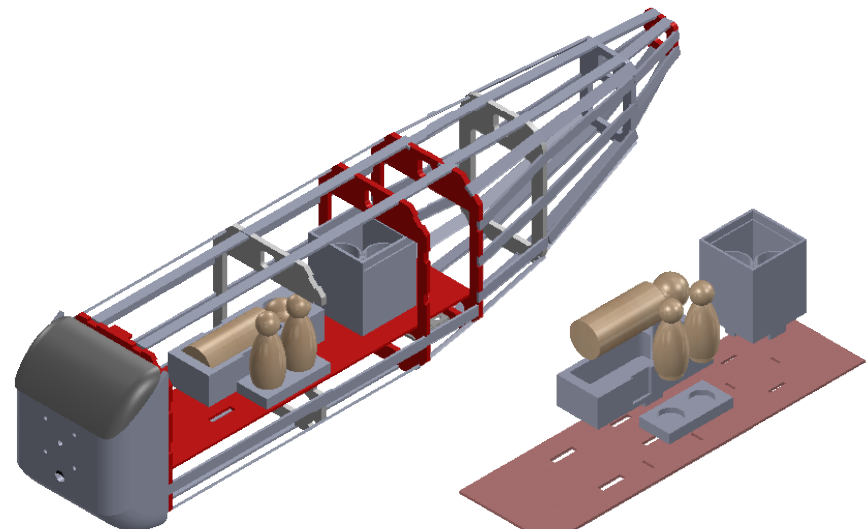
2

1

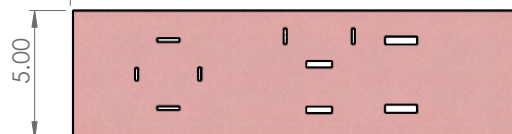
F

F

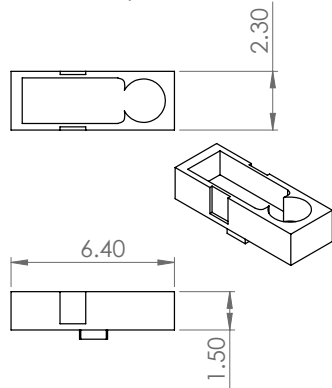
Mission 2 Configuration



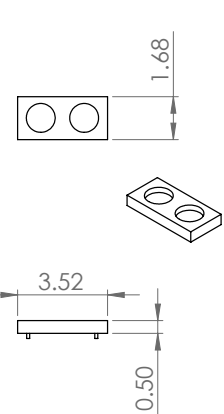
17.50



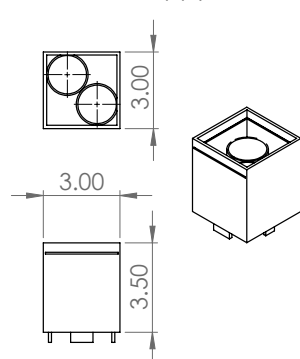
Gurney



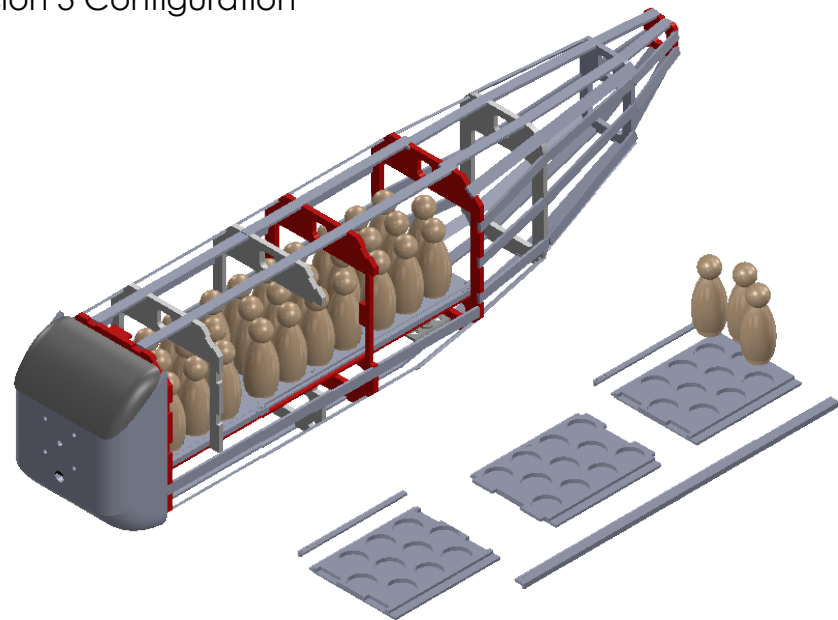
EMT Restraints



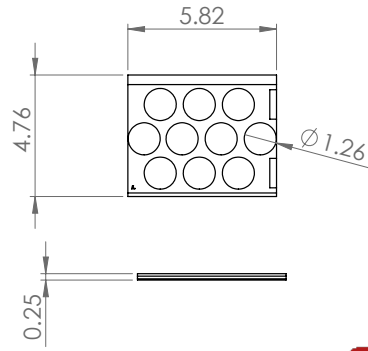
Medical Supply Cabinet



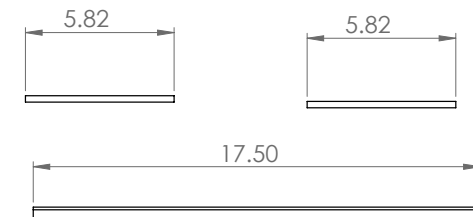
Mission 3 Configuration



Passenger Inserts



Insert Guiderails



Cornell University Design Build Fly



ALL RIGHTS RESERVED BY CORNELL UNIVERSITY DESIGN BUILD FLY

DRAWN BY:  
Will CoombsCHECKED BY:  
Adrian Lee

WEIGHT: M2 9.65 lbs M3 8.9 lbs

SCALE: 1:5

DATE: 2/10/2024 REVISION 2/14/2024

Cornell University

TITLE:  
**Payload Accommodation**313 Campus Rd. Ithaca,  
New York 14853

A3

ALL UNITS ARE IMPERIAL [IPS]

NOTE: All dimensions  
are given in  
inches or degrees

## 6 Manufacturing Plan

### 6.1 Manufacturing Process

The team has a manufacturing process resembling that of the Design Build Fly iteration cycle. The process goes through different phases, starting with modeling, then fabrication, then subsystem and system assembly, and ending with analysis and testing. This is depicted in Figure 6.1.1. After the competition rules were released, sizing and scoring analysis is performed to determine what parameters to optimize for the competition. After this optimization along with the initial conception of design, CAD models are developed using SOLIDWORKS to visualize how components would operate and integrate with one another. When completely designed and reviewed, the models enter the fabrication stage where they are converted into .dxf files to be laser cut, or .stl files to be 3D-printed.

All manufactured parts, along with externally purchased components, are then moved along into the system/subsystem assembly phase, where they are assembled into their respective subsystem components. Materials such as balsa, basswood, resin, carbon fiber, and other electrical components are integrated using epoxy, cyanoacrylate glue, wood glue, heat shrink tubes for wiring, or hardware fasteners including nuts, bolts, and screws. MonoKote, a smooth and continuous film, is used when necessary to cover subsystems/components that heat shrinks using a heating iron and a heat gun. During integration, if subsystems are not able to integrate smoothly, it may become necessary to revert back to component assembly, cycling back through the assembly process. This cycle is repeated multiple times in order to iterate on the most effective mission-based aircraft, with mission mechanisms being included in this process as well.

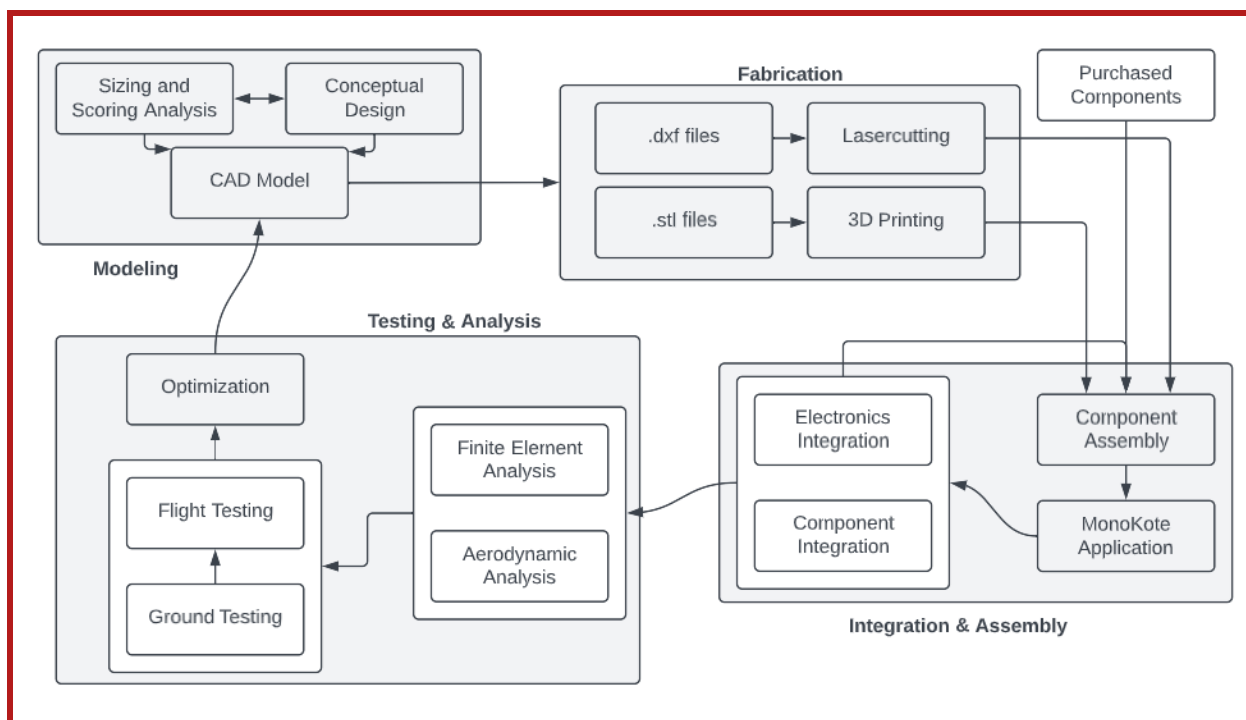


Figure 6.1.1: Manufacturing Flow Chart

## 6.2 Manufacturing Processes Investigated

Various manufacturing processes were considered for the build-up of the aircraft. The wings, empennage, fuselage, and mission-specific payloads and integration systems have various parameters that need to be considered while manufacturing. The following sub-section outlines some of these processes.

### 6.2.1 3D Printing

3D-printing allows for the fabrication of highly-complex parts not easily replicable. CUDBF has access to the Cornell University Rapid Prototyping Lab (RPL), which houses several 3D printers that can be loaded with materials such as PLA, ABS, resin, and Onyx filament (a nylon-based filament with chopped carbon fiber). Figures 6.2.1 show some of the printers used for manufacturing.



(a) Stratys F370 ABS 3D Printer



(b) Fortus 250mc PLA 3D Printer



(c) FormLabs 3+ Resin 3D Printer



(d) Markforged Mark Two Onyx 3D Printer

Figure 6.2.1: The 3D-printers CU DBF uses. All of these printers are located in the Cornell Rapid Prototype Lab.

### 6.2.2 Laser Cutting

With the majority of the aircraft consisting of primarily balsa and basswood, there are many precise parts that need to be cut. CUDBF utilizes the laser cutters in the RPL to ensure that parts are cut with pinpoint accuracy. The laser cutter shown in Figure 6.2.2 is able to cut large areas (36.00 inches x 24.00 inches) of wood up to a 1/4 inch thick, making it an extremely valuable asset for the team.

### 6.2.3 Adhesives

There are four different adhesives used to manufacture the aircraft: cyanoacrylate glue (CA), wood glue, epoxy, and Velcro. CA is used to permanently bond balsa wood-to-balsa wood, including ribs and stringers. Wood glue serves as a stronger adhesive, useful when attaching other types of wood together (balsa-to-basswood, basswood-to-basswood). Epoxy is used to attach plastic and composite components together. Finally, Velcro is used as a temporary adhesive for objects that need to shift around, namely, for the fuselage hatch, battery attachment, and M2 attachment.

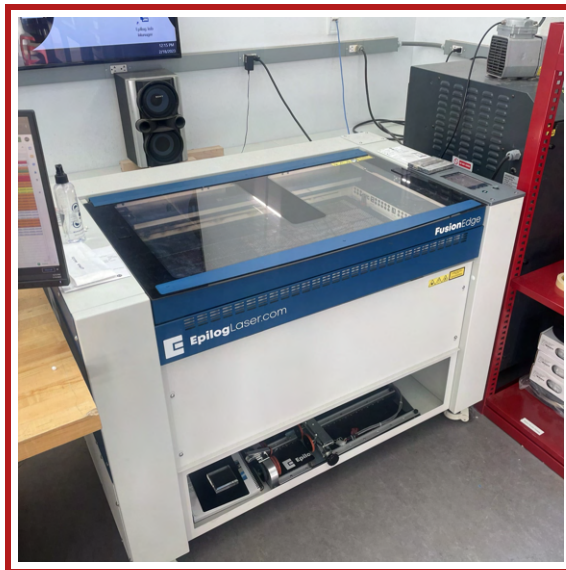


Figure 6.2.2: Cornell Rapid Prototyping Lab's Epilog Laser FusionEdge

## 6.3 Subsystem Manufacturing

### 6.3.1 Wing Manufacturing

The structurally critical main wing and control surface ribs, leading and trailing edge stringers, and servo and control plates are laser-cut from 1/8 inch basswood, while additional ribs were laser-cut from 1/8 inch balsa wood. The ribs and stringers were attached using wood glue for the main wing and flaperon control surfaces separately. Additional stringers were manually cut from balsa and attached, spaced along the main rib chord. A laser-cut basswood plate was glued between two ribs in each main wing and flaperon near the center of each half wing spanwise in order to hold servo attachments. Servos for each flaperon were glued to an acrylic plate using epoxy and which was then screwed into the wing's basswood plate. At the front of each wing control surface, polystyrene foam was glued to the control surface comb. Each wing and control surface was subsequently covered in a layer of MonoKote.

Control horns were screwed to the underside of each flaperon basswood plate. The servos were zeroed and then metal control rods were manually cut and then attached from the servo horn on each wing and control horn on each control surface. Each flaperon was connected to a wing surface using a hinge point glued into holes in the control surface on one side and the main wing rear comb and balsa block on the other side.

After this, the wings and integration piece were inserted onto the carbon fiber spar. The wood structure of the wing and partially MonoKoted surfaces are displayed in Figure 6.3.1. Note that the design for this iteration of the wing had separate flap and aileron surfaces and no hinge points.

### 6.3.2 Empennage Manufacturing

The stabilizer and control surface combs, ribs, stringers, and servo and control plates were laser-cut from 1/8 inch basswood. Ribs and stringers were made from 1/8 inch balsa wood. Assembling the vertical and horizontal stabilizers separately, ribs, combs, and stringers were attached using wood glue. The trailing edge balsa pieces were attached to the control surface airfoils using CA. Balsa blocks were glued behind the pin holes using wood glue and then drilled through completely. The horizontal stabilizer was then attached to the top of the vertical stabilizer using wood glue.



Figure 6.3.1: Wing structure before monokoting

EcoPower 640T servos for each control surface were glued to acrylic plates using epoxy and then those plates were screwed into the basswood plates in the stabilizers. The empennage at this stage of manufacturing is shown below in Figure 6.3.2.



Figure 6.3.2: Combined vertical and horizontal stabilizers with servos attached

### 6.3.3 Fuselage Manufacturing

The fuselage has a semi-monocoque structure with wooden ribs attached to a carbon fiber spar. The bulkhead rib, ribs supporting the wing, and rearmost rib were laser cut out of 1/8 inch thick basswood. The remaining ribs were laser cut out of 1/8 inch balsa wood. The nose cone was 3D-printed out of Onyx using a Markforged 3D-printer at the RPL. The stringers connected to the ribs were made of 1/8 inch thick balsa cut into 1/2 inch wide strips. The base plate was laser cut out of 1/8 inch thick basswood. During assembly, the fuselage ribs were lined up on the carbon fiber spar and then glued in place with wood glue. The stringers were then glued in place. Screws and glue were used to connect the nose cone and fuselage. The fuselage was also wrapped with MonoKote and run over with a sealing iron and then a heat gun.

The front landing gear is made from an aluminum strut and lever with springs to help absorb shock. Two foam



Figure 6.3.3: M2 fully printed and integrated into the fuselage baseplate.

wheels are attached to the bottom of the nose gear. To enable steering capabilities, a servo is connected to the top of the nose gear by a 3D-printed PLA socket. The PLA socket is connected to the base plate by 1/4 inch -20 x 2.50 inch carriage bolts with lock nuts and washers. The main gear is composed of 2.00 inch foam wheels that are screwed into a carbon fiber frame. The top of the carbon fiber frame is secured to the base plate with a 3D-printed PLA integration piece and 1/4 inch -20 x 2.00 inch hex bolts with lock nuts and washers.

#### 6.3.4 Mission Packages Manufacturing

**Mission 2** Due to the nature of the M2 payload, only a few viable options were available for manufacturing this component. The decision was made early on to use 3D-printing as it would allow rapid prototyping of precise parts. After this, the decision on materials was limited due to what could work with the printers. After testing different materials, ABS plastic was the best choice because the material was resistant to warping from the press-fit that are required for our design. Using PLA plastic would work initially, but the parts would warp under the stress of a press-fit.

All components were printed on Stratasys F170 or F370 printers at the RPL, which allows for free manufacturing. All components were manufactured with notches extruding from the bottom of the component so they can easily slot into pre-cut holes in the fuselage. Additionally, space for Velcro tape was added to the bottom of every component to provide additional support and eliminate any movement. The gurney also has spaces specifically cut out for a Velcro strap that is used to secure our patient. The MSC unit has a small slot at the top in order to cover our weights with a thin cut piece of balsa.

**Mission 3** Due to the exact dimensions, tolerances, and precision required by the press fit for Mission 3, it was decided early to use 3D-printers to manufacture the necessary parts. All parts of M3 were manufactured using 3D-printing with ABS material. This was done on a Stratasys F170 or F370 printer at the RPL. The first prototype was printed using PLA material, but the Passengers warped the holes they were in, causing the press fit to be loosened beyond repair. Because ABS is higher quality and not subject to the same sort of bending, it was decided that only ABS would be used in order to preserve the press fit. ABS was also chosen over other materials (such as resin or Onyx) because it was lighter and all of the mission parts could be printed on the same bed and save time. The

side rails were attached to the fuselage using epoxy. The inserts will slide in and out of the rails, so no bonding is necessary.

For restraints, two methods were combined to prevent Passenger movement during flight. First, an adhesive rubber sheet was used to provide extra friction against the bases of the Passengers. It was cut into 0.20 inch strips and placed inside the cutouts along the edge of the circle. The rubber sheet was purchased from Amazon. A wooden lattice was also made and was based off the CAD for the inserts. The locations of the cutouts were cut into a thin piece of balsa wood. This lattice was placed over the Passengers to ensure they remained secure. Since it must fit inside the hatch, the lattice was cut to match the fuselage width.



Figure 6.3.4: Finalized ABS insert for middle section of fuselage with passengers

### 6.3.5 Electronics Hatch Manufacturing

The electronics integration piece was 3D-printed for ease of manufacturing and increased precision. Although Onyx offers a higher melting point, ABS was selected for its lower cost and sufficient temperature tolerance. Velcro was cut to the size of the component slots and adhered in place, allowing the electronic components to be securely held in the integration piece, while remaining removable.

## 6.4 Manufacturing Milestones

A Manufacturing Gantt Chart was created to keep track of important milestones during the manufacturing phase. Each subteam kept track of the anticipated and actual manufacturing process of different components. Figure 6.4.1 shows the Manufacturing Gantt Chart used for the 2023-2024 Design, Build, Fly cycle.

# 7 Testing Plan

## 7.1 Subsystem Tests

### 7.1.1 Static Thrust Test

The static thrust test allowed for the verification of simulated eCalc values, ensuring the motor setup could maintain the thrust necessary to power the aircraft over the course of each mission. To test a wide array of configurations, three different propellers were used: 13.00 inch x 13.00 inch, 13.00 inch x 11.00 inch, 15.00 inch x 8.00 inch. For each propeller, the first trial set throttle to 100% simulate takeoff and the second trial set throttle to 60% to simulate cruising speed. Each trial was conducted with a fully-charged battery for consistency. A wattmeter was connected in

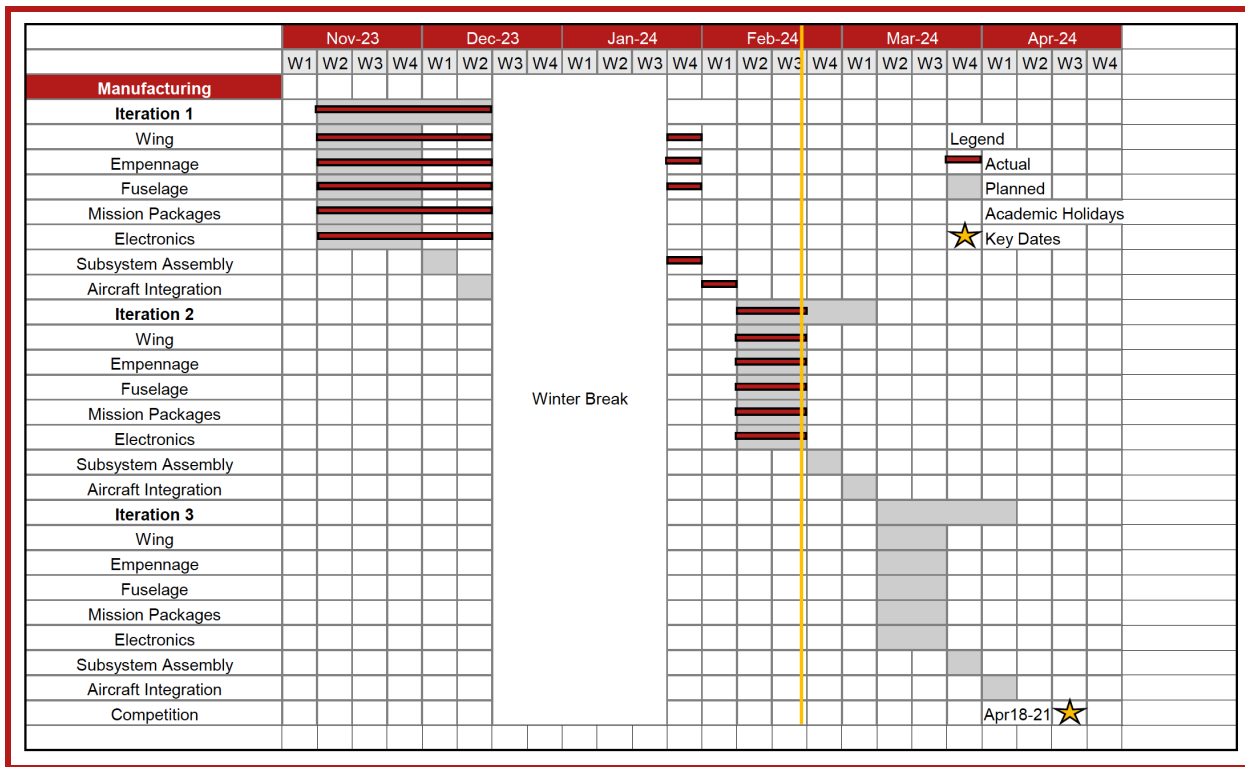


Figure 6.4.1: Gantt Chart of Planned and Actual Manufacturing Timeline

series between the ESC and battery to measure the current draw. The current draw was used to verify the current draw and fuse selection for Ursula Major.

The testing rig consisted of an L-shaped bar placed on a freely rotating axle. The motor mount, motor, and propeller were attached to the upper end of the bar, while the lower end was placed perpendicular to the ground on an electronic scale. The propeller's rotation creates a moment around the L-bar axle, while the lower end of the bar presses down on the scale. Since the two arms of the L bar are equal in length, the mass measured by the scale multiplied by the force of gravity is equal to the thrust generated. For safety, the test was conducted outside and all crew members involved were situated behind the propeller. Figure 7.1.1 shows the testing setup for static thrust tests.

### 7.1.2 Wingtip Tests

Before every scheduled flight test, the team conducted wingtip tests for the purposes of structural verification. The tests involved suspending the aircraft from the ground by its wingtips and attempting to balance the aircraft slightly before the quarter-chord of the wings, where the aerodynamic center lies. This was done such that the center of gravity for the empty weight, as well as the loaded weight of the aircraft, is marked for the competition. Additionally, the lateral mass distribution and symmetry of the aircraft were tested by balancing the aircraft by the motor axis and the tail spar. Similarly to the wingtip test, the necessary mass adjustments were noted in order to achieve the desired symmetry during flight testing.

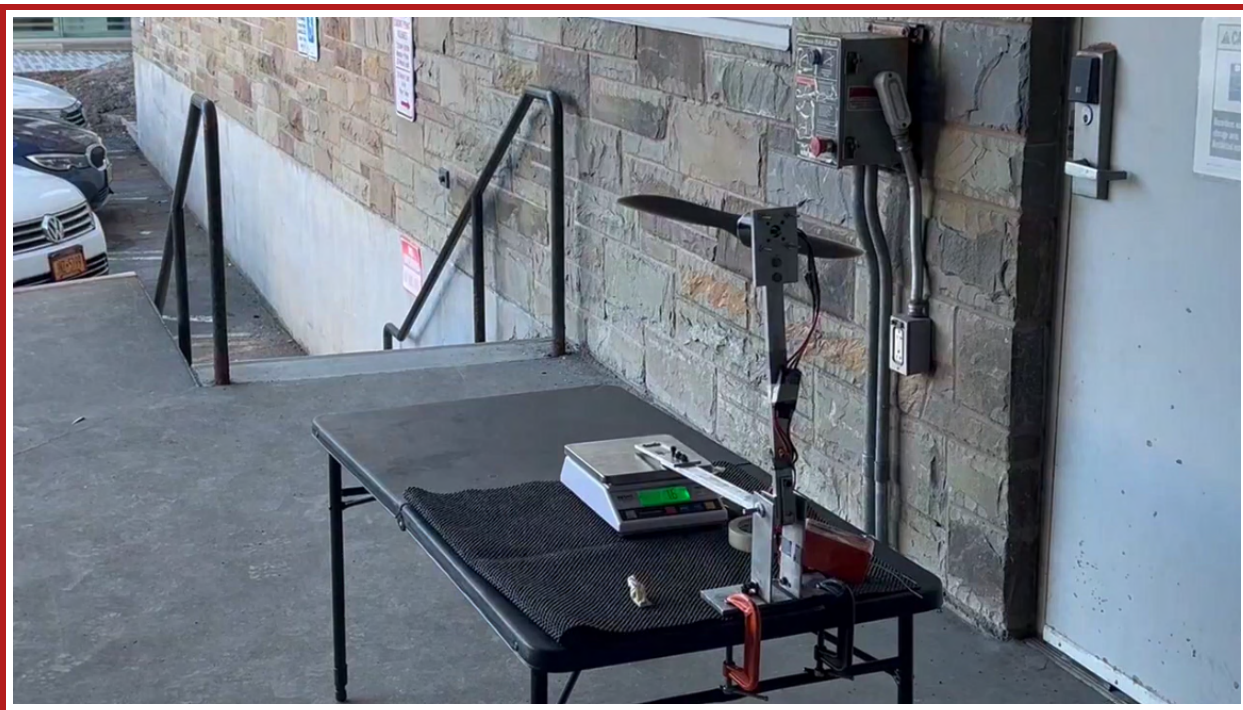


Figure 7.1.1: Static Thrust Testing Setup

## 7.2 Flight Testing Plan

The aerodynamics and controls subteam intends to conduct flight tests of the three iterations of the aircraft, including conducting wingtip and taxi tests right before each flight test. The purpose of these tests is to observe how well the aircraft performs under conditions akin to the AIAA Design Build Fly competition objectives, in reference to preliminary analyses. This will allow the team to make necessary changes for the next iteration based on the data collected from the tests. Due to time constraints, the team's goal was to conduct a flight test as soon as the construction of an iteration was completed. On February 6th, the team conducted the first flight test for the aircraft at a facility provided by the Ithaca Radio Control Society, where it was flown without payload. A wingtip test and taxi test were also conducted. The results of these tests are described in Section 8. The two other planned flight tests will take place sometime during the fourth week of February and the fourth week of March. For the second flight test, the team plans to observe how the revised aircraft would perform if it were to complete a lap under the conditions set by M2. A month later, the team will conduct the final flight test and analyze how the aircraft performs if it were to complete a lap under the conditions set by M3.

While the team will be observing the aircraft's performance during flight testing, the RC pilot shall give the team feedback on what they experienced when controlling the aircraft. The team will then use that feedback to modify the aircraft's design accordingly.

## 7.3 Flight Test Checklist

The following flight test checklist is used by the team to ensure the safety and preparedness for flight tests:

# Pre-Flight Checklist

Last Updated: Feb, 2024

Flight Test Date: \_\_\_\_\_



Task	✓	Remarks
Electrical Power Sources		
Verify Main Propulsion Battery at full charge		
Verify Receiver Battery at full charge		
Verify Transmitter Battery at full charge		
Aeronautics		
Verify wings are well secured to the fuselage		
Identify location of center of gravity		
Wingtip test		
Actuation		
Zero servos		
Correct servo connections to receiver, battery and ESC		
Ensure servos are securely fastened		
Verify control surfaces have enough deflection		
Propulsion		
Ensure correct propeller is mounted		
Ensure propeller is securely fastened		
Ensure we are using a Right (not Left) propeller		
Miscellaneous Tests		
Landing Gear/Roll Test		
Propulsion Mount Structural Test		
Transmitter Range Test		
Record total prop weight and total plane weight		
Flight Contingency Case Manifest		
LiPo Protective Bag	Y	
Electrical Tape, Duct Tape, Hinge Tape	Y	
Scissors, Xacto Knives (2)	Y	
Hand Drill and Drill Bits	Y	
CA Glue (2, Instant and Gap Filling) and Extra Tips	Y	
Balsa sheet (1/8, 1/16), balsa stringers	Y	
Extra Transmitter, Receiver, ESC	Y	
Thermal Blanket for Cold Weather		
2x sets of Allen Keys	Y	
Bolts and Nuts	Y	
Logistics		
Ensure weather conditions favorable		
File for FAA approval		

## Pre-Takeoff Checklist

Task	✓	Remarks
50% Throttle, Throttle Closed, Full Up Elevator, Full Right Rudder, Full Right Aileron		
Radio Failsafe set, Arming plug in possession		
Propeller rotating in correct direction		
Favorable Wind, Weather Conditions		

## 8 Testing Results

### 8.1 Subsystem Test Results

#### 8.1.1 Static Thrust Test Results

For the first round of testing, the Planet Hobby Joker 5060-7 motor was used. During flight tests, however, the torque from the motor resulted in a counterclockwise roll. The decision was made to switch to the smaller, Cobra 4120/22 motor for its potentially larger thrust output due to its higher kV rating. A 15.00 inch x 8.00 inch propeller was used in tandem with the new motor to investigate the potential benefits of the new configuration. Following the testing, the team settled on the 15.00 inch x 8.00 inch propeller and the Cobra 4120/22 motor for the flight time and thrust they provided.

Motors	Propellers	Max Thrust (lbs)	Flight Time (minutes)
Planet Hobby Joker 5060-7 370kV	13 inch x 13 inch	5.73	3.5
	13 inch x 11 inch	6.17	3.9
Cobra 4120/22 430kV	15 inch x 8 inch	8.16	7.5

Table 8.1.1: Static Thrust Test Results

### 8.2 Flight Test Results

During the first flight test, on February 6th, the aerodynamics and controls subteam successfully conducted various tests. The wingtip test allowed the team to observe and correct the longitudinal balance of the aircraft. The team observed that the aircraft was slightly longitudinally unstable, and would tend to tip backward on the ground if given a push from the front. Nonetheless, the team proceeded with preparations for the flight test. During the flight test preparations, the flaps ceased to function. This was due to contact interference between the aileron and flap dowel rods of the Iteration 1 design, which caused one of the servos controlling the flaps to burn out. Thus, both flaps were disabled and secured to the wing using adhesive tape. Before the flight test, the team conducted a short taxi test, which was successful. The aircraft was fully controllable on the ground, validating the landing gear design and indicating that the aircraft would be able successfully complete a takeoff roll. After the successful taxi test, the team moved forward with a flight attempt. During takeoff, the aircraft traveled roughly down the center line and was able to successfully lift off the ground after traveling about 45 feet. Immediately after lifting off, due to lateral instabilities and the overwhelming left-turning tendency of the motor, the aircraft rolled far to the left. The ailerons proved insufficient to return the aircraft to level flight, so the aircraft crashed a short while later.

During the flight test, initial performance expectations were not met by Iteration 1. Iteration 1 was expected to complete a lap under M1 conditions. Going into the flight test, there were various factors of uncertainty within the aircraft. Landing gear issues, flap failure, exceeding the mass budget, and lack of foam on the control surfaces were setbacks for Iteration 1. Despite the successful taxi test, the presence of these issues was revealed during flight test. Refinements within the design were proposed by the team to address these issues.

After gaining insight from the Iteration 1 tests, the aerodynamics and controls subteam reassessed the center of gravity and lateral stability modes of the aircraft using XFLR5. To increase stability, the team decided to increase the wingspan and the surface area of the ailerons. Additionally, the team pivoted to a hinge design to the flaperons to avoid deflection issues as outlined in 5. This change will also give greater control over the roll of the aircraft, allowing the pilot the ability to recover from any potential rolls that appear during flight. Lastly, it was discovered that the servos

used on Iteration 1 had insufficient torque to deflect the control surfaces into the oncoming flow. New servos with more power (64.00 oz-in, previously 20.80 oz/in) were found and will be used on future aircraft iterations.

Following these modifications, the team needed to further mitigate the swivel design limitation. The tail arm was increased, moving the tail back. This allows for the wing to swivel to be fully parallel to the fuselage. To account for new tail arm, the tail was resized. The chords of both the horizontal and vertical stabilizers were decreased, along with the span of the horizontal stabilizer.

In addition to increasing stability, the aerodynamics and controls subteam changed the materials used for some components from basswood to balsa wood to decrease the weight of the plane. Specifically, the ribs that are not structurally critical in both the wings and control surfaces were changed to balsa wood.

Lastly, the mechanical subteam also changed designs to decrease mass and improve overall ease of manufacturing.



Figure 8.2.1: Flight Test Preparation

## References

- [1] AIAA DBF Rules 2024. AIAA Foundation. Aug. 2023.
- [2] MATLAB. version 23.0.24 (R2023b). Natick, Massachusetts: The MathWorks Inc., 2023.
- [3] Snorri Gudmundsson. *General Aviation Aircraft Design*. Elsevier, Inc, 2014.
- [4] Tejas Dhekane and Nitin Sherje. "CFD Simulation of Different Taper Ratio Wings, Performing Trade-off Assessment and Development of A New Methodology to Plot Lift Distribution Curve and 3D Local Coefficient of Lift Distribution Graph". In: *International Journal Of Engineering Research And Technology* (2020).
- [5] A.L Bolsunovsky et al. "Flying wing—problems and decisions". In: *Aircraft Design* 4.4 (2001), pp. 193–219. ISSN: 1369-8869. DOI: [https://doi.org/10.1016/S1369-8869\(01\)00005-2](https://doi.org/10.1016/S1369-8869(01)00005-2). URL: <https://www.sciencedirect.com/science/article/pii/S1369886901000052>.
- [6] Gloria Stenfelt and Ulf Ringertz. "Lateral Stability and Control of a Tailless Aircraft Configuration". In: *Journal of Aircraft* 46.6 (2009), pp. 2161–2164. DOI: 10.2514/1.41092. eprint: <https://doi.org/10.2514/1.41092>. URL: <https://doi.org/10.2514/1.41092>.
- [7] URL: <https://www.tudelft.nl/en/ae/flying-v>.
- [8] S Ravikanth et al. "A Effect of Elevator Deflection on Lift Coefficient Increment". In: *International Journal of Modern Engineering Research* 5.6 (June 2015), pp. 09–25.
- [9] Daniel P. Raymer. *Aircraft Design: A Conceptual Approach*. American Institute of Aeronautics and Astronautics, 2021.
- [10] Perrine Pepiot. *3 Moment Equation FULL.pdf*. URL: [https://canvas.cornell.edu/courses/51470/files/7712098?module\\_item\\_id=1946094](https://canvas.cornell.edu/courses/51470/files/7712098?module_item_id=1946094) (visited on 02/20/2023).
- [11] Markus Mueller. *PROPCALC - the most reliable propeller calculator on the web*. Apr. 2017. URL: <https://www.ecalc.ch/motorcalc.php>.
- [12] Jeff Scott. *Aircraft Landing Gear Layouts*. 2023. URL: <https://aerospaceweb.org/question/design/q0200.shtml>.
- [13] Rudie Nagelmakers. *Engine Offset And Thrust Angle*. URL: <https://www.beetonrcflyers.ca/knowledge-base/engine-offset-and-thrust-angle>.